A THEORETICAL INVESTIGATION OF LOW ENERGY PROTON ON HYDROGEN COLLISIONS

A thesis
submitted in partial fulfilment
of the requirements for the Degree
of
Doctor of Philosophy in Physics
in the
University of Canterbury

by

J.K. Cayford

University of Canterbury
1976

CONTENTS

LIST OF FIGURES

LIST OF TABLES

ABSTRACT

The Proton on Hydrogen collision problem is treated in the time-dependent formalism using a new self-consistent nuclear trajectory model in conjunction with a simple semi-classical approximation. In this method the nuclear trajectory is dependent on the time-evolution of the electronic wavefunction which is described by a basis of H_2^+ eigenfunctions. The small-energy, large scattering angle region is well described in this way and agreement with available experimental data is obtained. The inclusion of the semi-classical approximation and the use of a larger molecular basis than hitherto employed allow these limits to be quite reasonably extended to describe the small angle and moderate energy region also.

Results of charge exchange probabilities and differential-scattering cross-sections in the range 150-1000 e.v. (lab. energy of incident proton beam) are presented along with some inelastic calculations on excitation into the Hydrogen 2p±1 and 2S states. It is further shown that the inclusion of the Gerade states (2Sσg, 3Dσg) in the basis set has a significant effect on the results obtained for collision energies of 700 e.v. and 1Kev.

A new numerical method is described which enables very rapid computation of all quantities required for the basis set, and leads to quick and simple integral calculations.

SECTION I

INTRODUCTION

The experimental work of Helbig & Everhart (Ref. 1) (which was verified and improved by Houver, Barat & Fayeton (Ref. 2)) with Proton and Hydrogen collisions, has led to many theoretical studies of this problem. The work of Bates et. al. (Refs. 3,4,5) are typical of earlier efforts where the nuclear motion was assumed to be classical and in straight lines (Impact Parameter Approximation, I.P.A.). This motion was treated as a perturbation on the electronic wavefunction which was solved in the Time-Dependent formalism.

The electronic wavefunction is usually described by a basis set of either atomic or molecular eigenfunctions of the stationary system; the technique being referred to as the method of Perturbed Stationary States (PSS). An expansion in molecular eigenfunctions is best used in the case of low energy collisions because, for a period of time in these collisions, the electron cannot be said to belong either to the target nucleus or to the incident nucleus. Obviously a large enough atomic basis set could describe such a situation but the time required for a computation would be very large.

The early results, using the I.P.A. and a two state molecular expansion ($1S\sigma g$, $2p\sigma u$) to describe the electronic motion, were in qualitative agreement with experiment but failed to predict with any accuracy either the heights

or the positions of the extrema in the charge exchange probability curves.

Bates & Williams (Ref. 5) found that including the effect of the rotation induced coupling between the $2p\sigma\mu$ and $2p\pi\mu$ molecular states gave much better quantitative agreement with experiment by damping and altering the phase of some of the theoretical charge exchange oscillations.

The E,θ range (where E is lab. energy of incident proton beam and θ is lab. frame scattering angle) where this particular approach gave best accord with experiment was $500 < E < 1000$ e.v., $\theta \approx 3^{o}$.

Explanations of the small angle, low energy deviations came from F.J. Smith (Ref. 6), Marchi & F.T. Smith (Ref. 7) and F.T. Smith (Ref. 8), who showed that the error was inherent in the classical nuclear path approximation. It is the quantum-mechanical or wave-effect of the nuclear motion which gives rise to almost all of the damping of charge exchange curves in this region. The theoretical results that lead to this conclusion are in fact present in the very early papers of Mott (Ref. 9) and of Massey & Smith (Ref. 10).

This effect has been taken into consideration in the work of McCarroll & Salin (Ref. 11) which has lead to the results published by McCarroll, Piacentini & Salin (Ref. 12). They have used an Eikonal approximation where the classical limit of the Time-Independent

Schrodinger equation for the whole system is coupled with the classical electronic transition amplitudes calculated in the I.P.A.. This work, along with the inelastic calculations of Chidichimo-Frank & Piacentini (Ref. 13) using the same method, are inaccurate in the moderate scattering angle region due to the straight line trajectory approximation. The high energy, large angle inaccuracies are caused firstly by high energy non-adiabatic effects appearing which are not described by a simple molecular basis set of three states, and secondly by failure to take any account of the bending of the trajectories at moderate to large scattering angles.

The first of these problems was first investigated by Bates (Ref. 3) who multiplied each of his molecular basis functions by a velocity dependent term to make the resulting functions eigenfunctions of the total system for infinite separations. This allows for the effect of the relative motion between colliding centres in the asymptotic limit. In part, these terms were to account for the so called "Momentum-Transfer" effects when the target electron was picked up by the incident proton. Rosenthal (Ref. 14) has pointed out that the introduction of these velocity dependent terms is purely to correct for the error caused by using a small basis set. Gaussorgues & Salin (Ref. 15) using an atomic basis set have shown that these velocity dependent effects are negligible below incident energies of 5 Kev.

The second problem, namely taking correct account

of the bending of the nuclear trajectories, is related to the first problem but becomes more important at low energies and moderate to large scattering angles. The difficulty surrounding the whole problem is understandable when the case of an inelastic transition is considered. If a Time-Dependent solution is attempted the difficulty is in correctly choosing classical trajectories for particular reaction channels, and for the Time-Independent equivalent, the difficulty lies in choosing a potential (since the wavefunction is changing in time then so too is the potential).

In the interesting paper of Knudson and Thorson (Ref. 16) a Time-Dependent method is presented where the electronic wavefunction is separated into a gerade half ($1S\sigma g$) and an ungerade half ($2p\sigma\mu$, $2p\pi\mu$), and each half is solved for along its own Time-Independent classical trajectory. However it was found that the "Inelastic phases" predicted by this approximation were inaccurate and had to be replaced by those calculated in a Time-Independent method. This particular Time-Dependent approach fails in the small energy, large scattering angle region due to the constant potentials used to solve for the nuclear motions. An explanation of this error is presented in the next few paragraphs.

Gaussorgues et. al. (Refs. 17 & 18) have presented a Time-Dependent method which relies on the physical reasoning that in large angle scattering, the scattering force is predominantly due to the repulsion between the

nuclear centres, and is comparatively unaffected by the changing electronic wavefunction.

It can be seen that this method has a lower limit because at small energies, despite the fact that large angle scattering may be involved, the nuclear scattering is significantly influenced by the way in which the electronic wavefunction evolves in time. This limit is illustrated in the paper (Ref. 18) where a discrepancy of 30% is noted for a scattering angle of 20° in a collision of 100 e.v. It is this small-energy, large to moderate scattering angle region which my method best describes.

To reiterate, the Eikonal Approximation using the I.P.A., (Ref. 11) accurately describes the small-energy, small scattering angle region where straight line classical behaviour and nuclear quantum-mechanical effects are predominant, whereas the Common-Trajectory method of Gaussorgues et. al. (Refs. 17 & 18) predicts accurately the experimental results in the small-energy, very large scattering angle regions where the nuclear-nuclear forces can be expected to provide for almost all of the scattering force. Neither of these two methods adequately describe the small-energy, moderate to large scattering angle region due to their not considering the mutual dependence between the electronic wavefunction and the nuclear trajectories. To elaborate; firstly, the solution of the electronic wavefunction is quite sensitive to variations in the bending of the classical trajectories, and secondly, the potential giving

rise to this bending is significantly dependent on the variations of the evolving electronic wavefunction.

To fill this gap I have developed a technique which solves for both the classical nuclear trajectory and the time evolution of the electronic wavefunction together in a self-consistent fashion.

The main approximation inherent in the method is the solution of the entire electronic wavefunction subject to the constraint of only one classical nuclear trajectory. In the Eθ range considered this approximation is reasonable as the classical trajectories associated with each contributing basis function do not differ markedly from the self-consistent trajectory. In addition, the "inelastic phase" predictions are quite accurate which is in contradistinction to the results of the dual-trajectory model proposed by Thorson et. al. (Ref. 16).

To facilitate the calculation of differential scattering cross-sections and to predict the low-energy, small angle damping in the charge oscillation curves previously mentioned, I have developed a semi-classical approximation which was derived from the work of Marchi & F.T. Smith (Ref. 7) and of F.T. Smith (Ref. 8). The contributing state electronic phases are introduced into this approximation from the solution of the electronic wavefunction along the self-consistent trajectory.

In the moderate energy region, where inelastic transitions (other than that to the $2p\pi\mu$ state) occur,

I have employed a molecular eigenfunction basis set which, at most, included the 1Sσg, 2pπμ, 2Sσg, 3pπμ, 2pσμ, 3Dπg, 3pσμ and 3Dσg states. The extra Gerard basis functions were included to account for any radially induced excitations present at higher energies, due to the neglect of velocity dependent translation factors in this work. It has been found that the inclusion of the states 2Sσg & 3Dσg in the basis set has a significant effect on the results for a collision energy of 1 Kev and gives better agreement with experiment than hitherto obtained. However, the neglect of any velocity dependent terms has led to some non-physical oscillations occuring which give rise to unreliable higher state excitation calculations.

In the next section the reasoning leading up to the self-consistent trajectory approximation is enlarged upon and the equations to be solved are derived. The semi-classical approximation and some theoretical justification for its use are presented in Section III followed by Section IV which deals with the numerical algorithm used to construct the basis set and also with some computational details of the problem. In Section V the results of this research are graphed along with those of several other theoretical approaches and experiments, and a discussion of the results is presented.

SECTION II

THE SELF-CONSISTENT TRAJECTORY

The basic premise implicit in all theoretical collision studies employing approaches along the lines of the PSS approximation, was presented in the half-century old work of Born and Oppenheimer (Ref. 19). The main reasoning behind that work is that if there are slow relative movements between nuclei in molecules (a slow ion-atom collision is an example of this) then the electronic wavefunction will adjust itself instantly to these movements since the electron moves so very much faster than the nuclei. This assumption is the basis of an approximation which is usually known as the zeroth-order Born Oppenheimer (B.O.) approximation since it is formally the result of truncating a perturbation expansion in $(\frac{m}{M})^{\frac{1}{4}}$ to the zeroth order term where m/M is the ratio of electronic to nuclear mass. When this approximation is applied to cases where the electronic wavefunction does not undergo transformations to higher states but instead alters itself to adjust to the slow nuclear movements, it is often referred to as the adiabatic approximation. If this B.O. approximation is applied to the collision problem, the total wavefunction becomes separable into a simple product of electronic and nuclear components. This separation leads to the method of solution where the solutions to the electronic equations are used to calculate an effective potential in which the nuclear motion may be solved.

Thus the total wavefunction may be written as,

$$\Psi(\bar{R},\bar{r}) = F(\bar{R})\psi(\bar{R},\bar{r}) \qquad (1)$$

where $\psi(\bar{R},\bar{r})$ is the electronic wavefunction and $F(\bar{R})$ is a function of the nuclear variables only. (All electronic and all nuclear coordinates are represented by $\bar{r}$, $\bar{R}$ respectively).

Mott (Ref. 9) showed that very little error was incurred in simple collision theory by assuming that the nuclei could be treated as infinitely heavy particles. This discovery led naturally to the Impact Parameter Approximation (I.P.A.) where the nuclei are treated as classical particles and travel undeviated at constant velocity along straight lines during an interaction.

When the I.P.A. is applied in solving the Proton on Hydrogen collision, the electronic wavefunction is usually expanded in a basis set of molecular eigenfunctions:

$$\psi(t,\bar{r}) = \sum_n a_n(t)\,\mu_n(t,\bar{r})\,e^{-i\int_o^t E_n(\tau)\,d\tau}$$

$$n = 1, 2, \ldots \text{ number of basis functions } N, \qquad (2)$$

where the a_n are time dependent coefficients and the E_n & μ_n are respectively, eigenenergies and eigenfunctions of the electronic Hamiltonian. The change in variable from $\bar{R}$ to t in the electronic wavefunction is because time is the independent variable in this approach and the nuclear coordinates, $\bar{R}$, may be extracted from the particular time-dependent straight-line trajectory chosen. Velocity dependent terms have here

been ignored for simplicity. This wavefunction is solved by substitution into the Time-Dependent Schrodinger equation;

$$H\psi(\bar{r},t) = i\hbar \frac{d\psi}{dt}(\bar{r},t) \quad , \tag{3}$$

where H is the electronic Hamiltonian of the system and is dependent on the internuclear separation R, but not on the time rate of change of R. Given the incident nucleus trajectory $\bar{R}(t)$, the problem is to solve for the electronic wavefunction after the collision is over in order to calculate the probability of charge transfer. It turns out that a simple superposition of the eigenfunctions 1Sσg & 2pσμ (μ_1 & μ_2) accurately gives the wavefunction of an electron in the 1S Hydrogenic state about the target nucleus for large internuclear separations, R. Thus:

$$\phi_{1S}(\bar{r}) = \frac{1}{\sqrt{2}}(\mu_1(R,\bar{r}) + \mu_2(R,\bar{r})) \tag{4}$$

is the ground state wavefunction of an electron centred about the target nucleus. Equation (3) is integrated in time subject to the initial conditions at t=0 that,

$$a_1 = 1/\sqrt{2} + i0 \quad \text{and,} \tag{5a}$$

$$a_2 = 1/\sqrt{2} + i0 \quad , \tag{5b}$$

where the subscripts 1 & 2 apply respectively to the

eigenfunctions 1Sσg & 2pσμ. It should be noted that the coefficients a_n are complex. The initial conditions (5) are chosen to correctly localize the electron around the target nucleus in the 1S Hydrogenic state.

When the substitution of (2) into (3) is carried out and if only a two state approximation involving states 1 & 2 is used (noting the orthonormality of the μ_n's),

$$\dot{a}_m(t) = 0 \quad , \; m = 1,2, \tag{6}$$

for all time and thus the solution of the wavefunction (2) is subject only to the evaluation of the terms;

$$e^{-i\int_o^t E_n(\tau)d\tau} \quad , \; n = 1,2 \tag{7}$$

along the particular straight line trajectory chosen. The solution of the problem is completed by using the inner product between the final wavefunction (2) and the wavefunction (4) to calculate the probability of charge exchange. This probability, P_{EX} is given by:

$$P_{EX} = 1 - |\langle\phi_{1S}|\psi(\infty,\underline{r})\rangle|^2 \quad , \tag{8}$$

since the term, $|\langle\phi_{1S}|\psi(\infty,\underline{r})\rangle|^2$ gives the probability that the electron stays on the target atom. Since the potential energy curves associated with states 1 & 2 are different (Appendix II), the two terms (7) will usually differ, which leads to a particularly simple partial explanation for the existence of the charge

exchange oscillations and qualitative agreement with experiment.

When a larger basis set is employed and if a transformation to the rotating centre of mass frame is carried out, equations (6) become;

$$\dot{a}_m(t) = \sum_n a_n(t)\left(i\dot{\theta}\langle\mu_m|\underset{\downarrow}{L_y}|\mu_n\rangle - V\langle\mu_m|\frac{d\mu_n}{dR}\rangle\right)e^{-i\int_o^t (E_n(\tau)-E_m(\tau))d\tau}, \tag{9}$$

$$\text{for } n = 1, 2, \ldots, N.$$

Dirac's Bra and Ket notation is used. Here $\theta(t)$ is the angular velocity of the rotating frame with respect to the lab frame, $V(t)$ is the time rate of change of the internuclear separation $R(t)$, and $\underset{\downarrow}{L_y}$ is the usual angular momentum operator. Equations (9) are integrated along a classical nuclear straight line trajectory while all dynamical variables and the internuclear separation at which the basis set is to be evaluated, are derived from that trajectory.

The rotation induced coupling is one of the most important mechanisms involved in predicting the experimental results and much work has been done to incorporate it into theoretical approaches to the problem.

Bates & Williams (Ref.5) and McCarroll, et. al. Refs. (12,29) have published work which includes the rotation coupling in an I.P.A. approach. However, the straight line trajectory approximation fails where large scattering angles are involved, as could be expected. The error introduced through not taking account of the

bending of the classical trajectories for collision energies in the range .1 - 1 Kev and scattering angles greater than 4^{o}, may be seen in the results published in (Refs. 12 & 18).

The physical reason explaining this error came from Knudson & Thorson (Ref. 16) who pointed out that the straight line trajectory samples the region of strong coupling (between $2p\sigma\mu$ & $2p\pi\mu$ states) much more than does the correct trajectory. The strong coupling region occurs for small internuclear separations (see integral graphed in Appendix II) and it is for such separations that the nuclear repulsive forces cause the incident nucleus to be at least partly repelled from the target leading to lesser coupling than that predicted by a straight line trajectory. One other difficulty involved with the I.P.A. is the ambiguity implied in obtaining a scattering angle from a straight line, particularly for large angles.

Bates & Sprevak (Ref. 20) have presented a method based on the work of Bates & Crothers (Ref. 21) which describes very large angle scattering and is very similar to the work of Gaussorgues et.al. (Ref. 17) discussed in the introduction. Bates & Sprevak in a Time-Independent approach have used for their potential an average of the $1S\sigma g$ & $2p\sigma\mu$ potentials, an approximation which fails in the low energy, moderate to large scattering angle region for the same reason as does the work of Gaussorgues et. al. (Refs. 17 & 18). The reason is that in this region it is no longer an accurate approximation

to calculate the potential which determines the nuclear motion regardless of the variations in time of the electronic wavefunction.

Knudson & Thorson (Ref. 16) have done some Time-Dependent calculations and though their results are good for small angles and small energies, the method is inaccurate for larger scattering angles because of the constant potential approximation used for the nuclear scattering. To obtain reliable results in the small-energy, moderate to large scattering angle region, a method is required which solves for both the nuclear motion and the electronic wavefunction without any constant potential approximations.

I have developed a method which meets these requirements where the incident nucleus is assumed to move along a single classical trajectory which has been found by using the time-evolution of the electronic wavefunction to give a time varying potential. The first step in obtaining a solution to a particular collision is to guess a probable nuclear classical trajectory given the initial conditions of incident energy, E and impact-parameter, ρ. The time-dependence of the electronic wavefunction is determined along the guessed trajectory using equations (5 & 9), and this time-dependence is used in calculating a time varying potential which leads to a better guess for the nuclear trajectory. The force on either the target or the incident nucleus at any time is given by:

$$F(t) = \sum_n |a_n(t)|^2 \frac{\partial E_n}{\partial R}(t) - \frac{1}{R^2} \quad . \tag{10}$$

The whole process is then repeated using the newly calculated trajectory and so on until the final electronic wavefunction obtained does not vary from iteration to iteration by more than a certain tolerance. As an indication of the speed of the method, I have found that for all collisions attempted, convergence to better than 1% was reached after only two iterations. Given an incident energy E, and an impact-parameter ρ, a calculation using the self-consistent trajectory method gives a scattering angle θ, and a solution to the electronic wavefunction (equation 2). For computational details involved in this section see (appendix I).

The results obtained as described may be used directly in the calculation of charge exchange probabilities as in eqtn. (8) but those results do not predict the low-energy, small to moderate angle damping which is experimentally observed and they do not directly lead to calculations of differential-scattering cross-sections (DSCS). To cover these inadequacies some effort must be made to include the quantum-mechanical effect of the nuclear motion.

SECTION III

THE SEMI-CLASSICAL APPROXIMATION

In theoretical investigations of experimental results it is important not to loose sight of the simple physical aspects of the problem considered. The observables associated with the proton on Hydrogen experiment are the incident beam energy E, and the scattering angle θ. In the straight-line trajectory studies of Bates et. al. (Refs. 3,4,5) a quantity ρ (the impact parameter) is introduced and placed on the same footing as accorded the experimental observables E & θ. Their method of solution is to decide upon the initial conditicns, ρ & E for a particular collision trajectory and these lead simultaneously to a unique solution of the electronic wavefunction and to a unique scattering angle θ . The physical implication of this model is that all protons observed to scatter through an angle θ result from identical collision trajectories, (each characterised by the same impact - parameter ρ) and possess the same observable electronic properties. An obvious example where this implication is not valid is the case of very low energy collisions ($\leqslant$ 15 e.v.) where the De Broglie wavelength of the incident proton is comparable to the spatial variation of the scattering potential. In such cases a wavepacket description of the incident proton is required as opposed to the classical point model.

In the energy range of interest (.1 to 1Kev) it is the zeroth order Born-Oppenheimer approx. (eqtn.1) which leads to the incorrect notion that there is a unique one-to-one dependence between ρ & θ for a particular collision energy E. It turns out that if the full quantal treatment of the problem is reduced to a semi-classical approximation, then the scattering observed at an angle θ may result from several different classical trajectories each characterised by the same angle θ. Thus, in a two state approximation using the $1s\sigma g$ & $2p\sigma\mu$ states, contributions to the scattering calculated at a particular scattering angle θ will generally come from two different classical trajectories, each characterized by its own impact parameter, ρ_1 & ρ_2 respectively. I shall now go through the reasoning which leads to this result. The works of F.T. Smith (Ref. 8) and of Marchi & Smith (Ref. 7) have contributed significantly to this section.

In a higher order approximation the total wavefunction is written:

$$\Psi(\bar{R},\bar{r}) = \sum_n F_n(\bar{R})\,\mu_n(\bar{R},\bar{r}),$$

$$n = 1, 2, \ldots, N, \qquad (10)$$

(where all variables are as before) instead of the approximation of eqtn. (1). If this wavefunction is affected by a scattering potential the resultant scattered wave is normally described by:

really asymptotic

$$\Psi_{total} = N^{-\frac{1}{2}} R^{-1} e^{ikR} \{ \sum_n f_n(\theta, E) \mu_n(R, r) \}$$

$$n = 1, 2, \ldots, N, \qquad (11)$$

where e^{ikR}/R is a spherical wave and the f_n's are the quantal scattering amplitudes. For simplicity eqtn. (11) is reduced to a two state expansion including the $1s\sigma g$ & $2p\sigma\mu$ states only:

$$\Psi_{total} = 2^{-\frac{1}{2}} R^{-1} e^{ikR} (f_1(\theta, E) \mu_1(R, r) + f_2(\theta, E) \mu_2(R, r)) \qquad (12)$$

The next step in the solution is to associate a physical quantity with these scattering amplitudes, thus:

$$\sigma_1(\theta, E) = |f_1(\theta, E)|^2 \qquad (13)$$

is known as the Differential Scattering Cross Section (DSCS) for scattering into state 1, and is an observable quantity. — how might it be observed?

Some necessary results and equations derived from the previous section are now presented. Rewriting eqtn. (4),

$$\phi_A = \frac{1}{\sqrt{2}} (\mu_1 + \mu_2) , \qquad (14A)$$

$$\phi_B = \frac{1}{\sqrt{2}} (\mu_1 - \mu_2) , \qquad (14B)$$

where ϕ_A & ϕ_B are ground state hydrogenic wavefunctions

centred around the target nucleus and the incident nucleus respectively. If the substitution,

$$\eta_n = - \int_o^t E_n(\tau) d\tau \ , \ n = 1, 2, \tag{15}$$

is put into eqtn. (7) then eqtn. (8) becomes,

$$P_{EX} = \tfrac{1}{2}[1 - \cos(\eta_1 - \eta_2)] , \tag{16a}$$

and

$$P_D = \tfrac{1}{2}[1 + \cos(\eta_1 - \eta_2)] \ , \tag{16b}$$

where P_D is the probability of direct scattering and $(\eta_1 - \eta_2)$ is referred to as the phase difference between states 1 & 2.

Following F.T. Smith (Ref. 8) the concept of the classical action is introduced. Given a particular scattering event whose classical trajectory is known there is a corresponding action,

$$S = \int \vec{P} . d\vec{q} \ , \tag{17}$$

where $\vec{P}(q)$ is the momentum along the trajectory. For the equivalent classical trajectory without interaction the action is,

$$S_o = \int \vec{P}_o . d\vec{q}_o \ , \tag{18}$$

which gives the overall collision action,

$$A = S - S_o \tag{19}$$

If a collision between two protons occurs subject only to a $^1S\sigma_g$ potential,

$$V_1(R) = E_1(R) - E_1(\infty) + 1/R^2 \tag{20}$$

the collision action along the resultant classical trajectory can be calculated. Given two such collisions derived from the $^1S\sigma_g$ & $^2p\sigma_u$ potentials, two collision actions A_1 & A_2 may be obtained. Marchi & Smith (Ref. 7) have shown that provided the scattering angles associated with the A_1 & A_2 are the same, θ_{scat} for example, then

$$(A_1 - A_2) = (\eta_1 - \eta_2) \ , \tag{21}$$

to second order in the function,

$$(V_1(R) - V_2(R))/E$$

where the V's are as defined in (20) and E is the collision energy. It should be noted that the classical phases (η's) used in eqtn. (21) were calculated using an average potential,

$$V_{avg} = \tfrac{1}{2}(V_1(R) + V_2(R)) \ , \tag{22}$$

to determine the nuclear motion and the scattering angle θ_{scat} , and not a straight line trajectory.

A simple physical explanation of the agreement shown in eqtn. (21) is given if eqtn. (17) is examined. The quantity $S/\hbar$ gives the number of De Broglie wavelengths along a particular classical trajectory and if two actions like A_1 & A_2 are combined the effect is very similar to the interference resulting from the superposition of two waves. Thus the combination of two totally classical quantities, i.e. action integrals, and the use of two contributing trajectories, leads to qualitative agreement with experiment by producing oscillations. Eqtn. (12) may be rewritten thus,

$$\Psi_{total} = e^{ikR}/2R((f_1 + f_2)\phi_A + (f_1 - f_2)\phi_B) \qquad (23)$$

using eqtns. (14), leading to the DSCS's for direct scattering and charge exchange,

$$\sigma_{EX} = \tfrac{1}{4}|f_1 - f_2|^2 \ , \qquad (24a)$$

$$\sigma_D = \tfrac{1}{4}|f_1 + f_2|^2 \ . \qquad (24b)$$

In approaches using the I.P.A. the predictions for probability of charge exchange P_{EX}, are undamped in the small-energy, small-scattering angle region (see eqtns. 16) whereas here,

$$P_{EX} = \frac{\sigma_{EX}}{\sigma_D + \sigma_{EX}} \ , \qquad (25)$$

can only be undamped if $|f_1| = |f_2|$.

The scattering amplitude f, is a quantum mechanical term but to be consistent with the correspondence principle, it should have a classical limit, let this be

$$f_{classical} = \exp(iA/\hbar) \ , \tag{26}$$

(using eqtn. (19)) since in the high-energy, or classical nucleus region, the charge exchange oscillations still exist and are predicted by eqtn. (26) but the nuclear quantum-mechanical damping is no longer present. If the full-quantal scattering amplitude is written:

$$f = \exp(iAq/\hbar) \tag{27}$$

then Aq may be expanded,

$$Aq = A + \hbar A_1 + \hbar^2 A_2 + \ldots \ , \tag{28}$$

and thus A is the classical limit of Aq and leads to eqtn. (26). However, since the quantal DSCS is given by $|f|^2$, then it would be reasonable to expect the classical approximation of f to lead to a classical DSCS. The classical DSCS is given by,

$$\sigma_c(\theta,E) = - \frac{\rho}{\sin\theta} \frac{\partial\rho}{\partial\theta} \tag{29}$$

as seen in Ref. (22), and if F is the classical approximation of f then would expect,

$$\sigma_c(\theta,E) = |F|^2 \qquad (30)$$

This is achieved by setting the imaginary part of A_1 to,

$$I_m(A_1) = \tfrac{1}{2} \log_e \sigma_c \ . \qquad (31)$$

(The real part of A_1 and its consequences is dealt with by Ford and Wheeler (Ref. 30), but it has no part in this research.) This gives, to first order in $\hbar$, a classical scattering amplitude,

$$F(\theta,E) = \sigma_c^{\frac{1}{2}} \exp(iA/\hbar) \ . \qquad (32)$$

The classical approximations to the f_1 & f_2 of eqtn. (12) may be written,

$$f_n(\theta,E) = \left(\frac{-\rho_n}{\sin \theta_n} \times \frac{\partial \rho_n}{\partial \theta} \right)^{\frac{1}{2}} \exp(iA_n/\hbar) \quad n = 1, 2, \qquad (33)$$

where the relationship between ρ_n & θ_n is determined classically using the potential $V_n(R)$ given by eqtn. (20). Since the potentials $V_1(R)$ & $V_2(R)$ are significantly different for some values of R, then so will be the terms, $\left(\frac{-\rho_n}{\sin \theta_n} \frac{\partial \rho_n}{\partial \theta} \right)$, n = 1, 2 and therefore, $|f_1| \neq |f_2|$ for certain collision trajectories. Thus the small-energy, small angle damping which is experimentally observed has a theoretical description.

In my calculations I have used eqtns. (21 & 33) combined with the solutions obtained for the electronic wavefunction in the self-consistent trajectory approximation,

to produce differential-scattering cross sections. Eqtn. (21) was obtained by Marchi & Smith (Ref. 7) using an average potential (eqtn. (22)) and hence its use here is justified since the self-consistent trajectory technique uses an average potential (eqtn. (10)a) to determine the nuclear motion. It is well known, (Bates & Sprevak (Ref. 20)), that the rotation induced excitation causes a change in the phase of the charge exchange oscillations calculated in the two state approximation. I have taken this effect into consideration by using the coefficients a_n (see eqtn. (2)) as corrections to the classical phases η_n. To obtain results as a function of the scattering angle θ, I solve for the electronic wave-function along many different self-consistent trajectories, all at the same collision energy E. Using eqtns. (21 & 33), the scattering amplitudes are written, for a particular energy,

$$f_n(\theta) = \left[\frac{-\rho_n(\theta)}{\sin\theta}\frac{\partial\rho_n(\theta)}{\partial\theta}\right]^{\frac{1}{2}} a_n(\theta)\exp(i\eta_n(\theta)),\ n = 1, 2, \ldots N \qquad (34)$$

where the $N^{-\frac{1}{2}}$ in eqtn. (11) may be dropped since $\sum_n |a_n|^2 = 1$. (It should be noted that the $\eta_n \neq A_n$ but that strict correctness is achieved when the phase differences are calculated in accordance with eqtn. (21)).

In higher energy collisions (E > 1Kev) it becomes possible to excite the electron to hydrogenic states other than the 1S and 2p ± 1 states. I have allowed for this by expanding the basis set to include the rotation induced excitation, $2p\pi\mu \rightarrow 3p\sigma\mu$ and $3p\sigma\mu \rightarrow 3p\pi\mu$.

These excitations provide for the possibility of describing scattering into the 2S and 3p±1 hydrogenic states respectively. The hydrogenic states 2S, 2p±1 and 3p±1 may be written,

$$\phi(2S)_{A,B} = \frac{1}{\sqrt{2}} (\mu(2S\sigma g) \pm \mu(3p\sigma\mu)) \tag{35a}$$

$$\phi(2p\pm)_{A,B} = \frac{1}{\sqrt{2}} (\mu(3D\pi g) \pm \mu(2p\pi\mu)) \tag{35b}$$

$$\phi(3p\pm)_{A,B} = \frac{1}{\sqrt{2}} (\mu(4D\pi g) \pm \mu(3p\pi\mu)) \tag{35c}$$

where the notation of eqtn. (14) is used. Large internuclear separations are required for eqtns. (35) to be accurate. In all calculations which I carried out the first molecular wavefunctions in the expansions (eqtns. (35)) were barely excited and were consequently neglected in higher state DSCS calculations. Since there is only one molecular state contributing to the excitation of each of the higher hydrogenic states then there is no interference between scattering amplitudes (as in eqtns. 24) and this leads to identical direct and exchange DSCS's. The differential scattering cross-sections for direct & exchange scattering into the higher states are written,

$$\sigma(2S)_{D,EX} = \tfrac{1}{2} \frac{\rho_3}{\sin\theta} \frac{\partial\rho_3}{\partial\theta} |a_3|^2 \tag{36a}$$

$$\sigma(2p\pm1)_{D,EX} = \tfrac{1}{2} \frac{\rho_4}{\sin\theta} \frac{\partial\rho_4}{\partial\theta} |a_4|^2 \tag{36b}$$

$$\sigma(3p\pm)_{D,EX} = \tfrac{1}{2} \frac{\rho_5}{\sin\theta} \frac{\partial\rho_5}{\partial\theta} |a_5|^2 \tag{36c}$$

where eqtn. (34) has been used and where 3,4,5 apply

respectively to the $3p\sigma\mu$, $2p\pi\mu$, and $3p\pi\mu$ molecular eigenfunctions. When the possibility of higher state excitations is included the probability of charge exchange represented by eqtn. (2) must be modified to,

$$P_{EX} = \frac{\sum_n \sigma_n^{EX}}{\sum_n \sigma_n^{D} + \sum_n \sigma_n^{EX}} \quad n = 1, 2, \ldots, N. \tag{37}$$

To complete this Section the final DSCS for scattering into the 1S state is written,

$$\sigma(1S)_{EX} = \tfrac{1}{2}\left| \left(\frac{-\rho_1}{\sin\theta} \frac{\partial \rho_1}{\partial \theta} \right)^{\frac{1}{2}} a_1 \exp(i\eta_1) - \left(\frac{-\rho_2}{\sin\theta} \frac{\partial \rho_2}{\partial \theta} \right)^{\frac{1}{2}} a_2 \exp(i\eta_2) \right|^2 \tag{38}$$

where eqtns. (34 & 24) are used and remembering the new normalization of eqtn. (34).

SECTION IV

THE BASIS SET

In most studies of the Proton on Hydrogen collision problem in the low-energy region (1< Kev), a basis set of molecular eigenfunctions has been used to describe the electronic wavefunction. A partial justification of this choice of basis set is the quasi-molecular nature of the system for low collision velocities at small internuclear separations. Examples of molecular basis set approaches may be seen in the works of Ferguson (Ref. 23), Bates & Williams (Ref. 5), Knudson & Thorson (Ref. 16) and McCarrol, Piacentini & Salin (Ref. 12).

The main problem associated with such a basis set is, to quote from Bates & McCarroll (Ref. 3) who first pointed it out, that though these eigenfunctions satisfy the appropriate equation for all internuclear separations if the internuclear velocity is zero, they do not satisfy it for all velocities of relative motion if the internuclear separation is infinite. This problem was partly solved by the introduction of certain velocity dependent terms and much improved theoretical results were obtained in the high energy region (see Ferguson (Ref. 23)). However Ferguson (Ref. 23) and Gaussorgues & Salin (Ref. 15) showed that the introduction of these velocity dependent terms had a negligible effect on the theoretical results obtained for collision energies below 1 Kev. They are neglected in this work.

If the velocity dependent terms are omitted the radial interaction connecting eigenfunctions of the same parity and angular momentum projection appears (see eqtn. 9). To allow for any possible excitations occuring because of this mechanism I have included in my basis set the even parity states, $2S\sigma g$, $3D\sigma g$ and the odd parity state $3p\sigma\mu$. The angular interaction term also shown in eqtn. (9) connects states whose parity is the same but whose angular momentum projections differ by 1. To describe any resulting rotational excitations the basis set has been extended to include the $3D\pi g$, $2p\pi\mu$ and $3p\pi\mu$ electronic states also. The basis set size was terminated here because preliminary results showed that the inclusion of higher states had a negligible effect on the charge exchange probability curves. (It will be seen in the next section that this termination led to errors in the calculations of excitations of higher states.)

The largest basis set used consisted of the following functions:-

$$\mu_1 = \psi(1S\sigma g)$$

$$\mu_2 = \psi(2p\sigma u)$$

$$\mu_3 = \psi(3p\sigma u) \qquad (37)$$

$$\mu_4 = \frac{1}{\sqrt{2}}(\psi(2p\pi u_+) + \psi(2p\pi u_-)$$

$$\mu_5 = \frac{1}{\sqrt{2}}(\psi(3p\pi u_+) + \psi(3p\pi u_-))$$

$$\mu_6 = \psi(2S\sigma g)$$

$$\mu_7 = \psi(3D\sigma g)$$

$$\mu_8 = \frac{1}{\sqrt{2}}(\psi(3D\pi g_+) + \psi(3D\pi g_-))$$

where the subscripts + & - apply to the angular momentum projection quantum number m = ±1. The summation in the π state basis functions is to satisfy the condition that there be no resultant angular momentum about the internuclear axis.

To calculate the quantities required by the time-dependent basis set a numerical technique developed by Cayford, Fimple & Unger (Ref. 24) for atomic calculations was applied by Cayford, Fimple, Unger & White (Ref. 25) to the H_2^+ two centre problem. The standard method of obtaining the eigenfunctions and eigenvalues of the H_2^+ system is to solve for the wavefunction using a truncated infinite series. Examples of such calculations may be seen in Refs. (26,27). The electronic wavefunction of the H_2^+ system is usually separated thus,

$$\psi = L(\lambda)M(\mu)(\exp(im\phi)/\sqrt{2\pi}) \quad , \tag{38}$$

where λ, μ and ϕ are the usual confocal elliptic coordinates,

$$\lambda = (r_a + r_b)/R$$

$$\mu = (r_a - r_b)/R \qquad (39)$$

(r_a & r_b are the distances from the two respective nuclear centres to the electron).

Peek (Ref. 27) using a series expansion has determined H_2^+ eigenfunctions (eqtn. (38)) to an accuracy of $1:10^{17}$ with 20 terms in μ and 16 terms in λ. Computing the value of one of the integrals given in eqtns. (9) using such an expansion would require the summation of approximately 10^5 analytic integrals. Even if an accuracy of $1:10^8$ was required the figure 10^5 would only be reduced by an order of magnitude. Using the numerical technique to be presented in this section, accuracies of $1:10^8$ can be achieved using at most 10^3 summations along with a numerical extrapolation.

The functions L & M of eqtn. (38) are solutions of,

$$\left[\frac{d}{d\lambda}(\lambda^2-1)\frac{d}{d\lambda} + A + \frac{ER^2\lambda^2}{2} + 2R\lambda - \frac{m^2}{\lambda^2-1}\right] L(\lambda) = 0 \ ,$$

$$\text{where } 1 \leqslant \lambda \leqslant \infty \ , \qquad (40)$$

and of,

$$\left[\frac{d}{d\mu}(1-\mu^2)\frac{d}{d\mu} - A - \frac{ER^2\mu^2}{2} - \frac{m^2}{1-\mu^2}\right] M(\mu) = 0 \ ,$$

$$\text{where } -1 \leqslant \mu \leqslant 1 \ . \qquad (41)$$

Equations (40) & (41) are solved subject to the boundary conditions,

$$L(\infty) = 0 \quad ,$$

$$L(1),\ M(-1),\ M(+1) \text{ are finite,} \tag{42}$$

and to the normalization conditions,

$$\int L^2 d\lambda = 1 \quad , \tag{43a}$$

$$\int M^2 d\mu = 1 \quad . \tag{43b}$$

(The correct normalization of ψ, namely that,

$$\frac{R^3}{8} \int L^2 M^2 (\lambda^2 - \mu^2) d\lambda d\mu = 1, \tag{44}$$

is corrected for at the end of the computation.) To remove the singularities which exist in eqtns. (40 & 41) due to the terms in m^2, the transformations,

$$\mathcal{L}(\lambda) = L(\lambda)/(\lambda^2 - 1)^{m/2} \tag{45a}$$

and

$$M(\mu) = M(\mu)/(1 - \mu^2)^{m/2} \tag{45b}$$

are made. These lead to the new equations,

$$\left[(\lambda^2-1)\frac{\partial^2}{\partial\lambda^2} + 2(m+1)\lambda\frac{\partial}{\partial\lambda} + A + \frac{ER^2\lambda^2}{2} + 2R\lambda + m(m+1)\right]\mathcal{L}(\lambda) = 0, \tag{46a}$$

and ,

$$\left[(1-\mu^2)\frac{\partial^2}{\partial\mu^2} - 2(m+1)\mu\frac{\partial}{\partial\mu} - A - \frac{ER^2\mu^2}{2} - m(m+1)\right]M(\mu) = 0 . \tag{46b}$$

The method used requires that the functions to be solved go to zero at their end points and to this end the transformations

$$X(\lambda) = (\lambda^2 - 1)\mathcal{L}(\lambda) \quad , \tag{47a}$$

and ,

$$Y(\mu) = (1 - \mu^2)M(\mu) \quad , \tag{47b}$$

are substituted into eqtns. (46) leading to,

$$\left[(\lambda^2-1)\frac{\partial^2}{\partial\lambda^2} + 2(m-1)\lambda\frac{\partial}{\partial\lambda} + 2\frac{(\lambda^2+1)}{(\lambda^2-1)} - \frac{4m\lambda}{\lambda^2-1} + A + \frac{ER^2\lambda^2}{2} + 2R\lambda + m(m+1)\right] X(\lambda) = 0 , \tag{48a}$$

and

$$\left[(1-\mu^2)\frac{\partial^2}{\partial\mu^2} - 2(m-1)\mu\frac{\partial}{\partial\mu} + 2\frac{(1+\mu^2)}{(1-\mu^2)} - \frac{4m\mu}{1-\mu^2} - A - \frac{ER^2\mu^2}{2} - m(m+1)\right] Y(\mu) = 0 . \tag{48b}$$

As these equations are to be solved numerically it is no longer feasible to use the λ coordinate system since it cannot be divided up into a finite number of finite mesh spaces. To eliminate this problem the λ space is transformed to another space whose limits are finite. When solving eqtn. (38) for the case of large internuclear separations, it is obvious that computational emphasis should be placed on those regions which are close to each nuclear centre. To deal with these two abovementioned problems, the following coordinate space transformations have been devised,

$$\xi = (\lambda-1)/(1+C(\lambda-1)) \quad ,$$

$$\text{where } 0 \leqslant \xi \leqslant 1/C \quad , \tag{49a}$$

and,

$$\rho = \mu/(A-\mu^2)$$

$$\text{where } -1/(A-1) \leqslant \rho \leqslant 1/(A-1) \quad , \tag{49b}$$

where A & C are constants dealt with later. Thus eqtn. (48a) after the substitution of eqtn. (49a) becomes,

$$\left|(2\xi+(1-2C)\xi^2)(1-C\xi)^2 \frac{\partial^2}{\partial\xi^2}\right.$$

$$+ \{2(m-1)(1+(1-C)\xi)(1-C\xi) - 2C(2\xi+(1-2C)\xi^2)(1-C\xi)\}\frac{\partial}{\partial\xi}$$

$$+\frac{2(2+(2-4C)\xi+(1-2C+2C^2)\xi^2)-4m(1+(1-C)\xi)(1-C\xi)}{(2\xi+(1-2C)\xi^2)}$$

$$+A+m(m+1)+\frac{ER^2(1+(1-C)\xi)^2}{2(1-C\xi)^2}+\frac{2R(1+(1-C)\xi)}{1-C\xi}\Bigg]X(\xi)=0\ . \tag{50}$$

Similarly eqtn. (48b) becomes,

$$\Bigg[\frac{\rho^2(1+4A\rho^2)(4\rho^2-(\sqrt{1+4A\rho^2}-1)^2)}{(\sqrt{1+4A\rho^2}-1)^2}\frac{\partial^2}{\partial\rho^2}$$

$$+\Bigg\{\frac{2\rho(4\rho^2-(\sqrt{1+4A\rho^2}-1)^2)(\sqrt{1+4A\rho^2}^3-(1+6A\rho^2))}{(\sqrt{1+4A\rho^2}-1)^3}$$

$$-2(m-1)\rho\sqrt{1+4A\rho^2}\Bigg\}\frac{\partial}{\partial\rho}+\frac{2(4\rho^2+(\sqrt{1+4A\rho^2}-1)^2)-8m\rho(\sqrt{1+4A\rho^2}-1)}{4\rho^2-(\sqrt{1+4A\rho^2}-1)^2}$$

$$-\frac{ER^2(\sqrt{1+4A\rho^2}-1)^2}{8\rho^2}-A-m(m+1)\Bigg]Y(\rho)=0\ . \tag{51}$$

The boundary conditions (42) are now given by,

$$X(0),\ X(1/C),\ Y(-1/(A-1)),\ Y(1/(A-1)=0\ , \tag{52}$$

and the normalization conditions (43) are,

$$\int X^2\left(\frac{(1-C\xi)^2}{2\xi+(1-2C)\xi^2}\right)^{(2-m)}\frac{1}{(1-C\xi)^2}\,d\xi=1 \tag{53a}$$

and

$$\int Y^2\left(\frac{4\rho^2}{4\rho^2-(\sqrt{1+4A\rho^2}-1)^2}\right)^{2-m}\frac{(\sqrt{1+4A\rho^2}-1)}{2\rho^2\sqrt{1+4A\rho^2}}\,d\rho=1 \tag{53b}$$

Equations (50-53) are now translated to finite difference form. The whole ξ space is divided up by a mesh of N-1 evenly spaced mesh points giving the interval between points, $h_1 = 1/CN$. A similar treatment of the ρ space leads to a mesh spacing $h_2 = 2/((A-1)N)$. The following notation will be used,

$$\xi_k = kh_1 \quad , \; k = 0, 1, \ldots , N$$

$$X_k = X(\xi_k)$$

$$\rho_k = -1/(A-1) + kh_2 \quad k = 0, 1, \ldots , N \tag{54}$$

$$Y_k = Y(\rho_k) \quad .$$

A first order approximation to the derivatives in eqtns. (50,51) is used. As examples of this approximation derivatives of the function X at the mesh point k are presented,

$$\left.\frac{dX}{d\xi}\right|_{\xi_k} \approx \frac{1}{2h_1} (X_{k+1} - X_{k-1}) \quad , \tag{55a}$$

and

$$\left.\frac{d^2X}{d\xi^2}\right|_{\xi_k} \approx \frac{1}{h_1^2} (X_{k-1} - 2X_k + X_{k+1}) \tag{55b}$$

The integrals (eqtns. 53) are approximated by trapezoidal rule which is entirely consistent with the first order

approximations of the derivatives.

To illustrate the finite difference form, eqtns. (50,52,53) are put into this form. Thus, at each internal mesh point in ξ we have the following set of equations,

$$\cdot\left[-\frac{2k(2+(1-2C)kh_1)(1-Ckh_1)^2}{h_1}+A+m(m+1)+\frac{ER^2(1+(1-C)kh_1)^2}{2(1-Ckh_1)^2}\right.$$

$$+\frac{2(2-(2-4C)kh_1+(1-2C-2C^2)k^2h_1^2)-4m(1+(1-C)kh_1)(1-Ckh_1)}{(2kh_1+(1-2C)k^2h_1^2)}$$

$$\left.+\frac{2R(1+(1-C)kh_1)}{1-Ckh_1}\right]X_k+\frac{k(2+(1-2C)kh_1)(1-Ckh_1)^2}{h_1}\ (X_{k-1}+X_{k+1})$$

$$+\left[\frac{(m-1)(1+(1-C)kh_1)(1-Ckh_1)-C(2kh_1+(1-2C)k^2h_1^2)(1-Ckh_1)}{h_1}\right]\ x$$

$$(X_{k+1}-X_{k-1})=0\ ,$$

$$k=1,\ \ldots,\ N-1 \qquad (56)$$

This is a set of N-1 equations in the unknowns $X_k(k=0,1,\ \ldots,N)$ and also the energy E and separation constant A. A similar set of equations in the unknowns $Y_k(k=0,\ 1,\ \ldots\ ,\ N)$, E & A may be written using eqtn. (51). The normalization conditions become,

$$h_1\sum_{k=1}^{N}\left[\frac{(1-Ckh_1)^2}{2kh_1+(1-2C)k^2h_1^2}\right]^{(2-m)}\frac{1}{(1-Ckh_1)^2}\ X_k^2-1=0, \qquad (57a)$$

and,

$$h_2 \sum_{k=1}^{N} \left(\frac{4(-B+kh_2)^2}{4(-B+kh_2)^2-(\sqrt{1+4A(-B+kh_2)^2}-1)^2} \right)^{(2-m)} \quad x$$

$$\frac{(\sqrt{1+4A(-B+kh_2)^2}-1)}{2(-B+kh_2)^2\sqrt{1+4A(-B+kh_2)^2}} Y_k^2 - 1 = 0 \ , \qquad (57b)$$

where $B = 1/(A-1)$.

It should be noted that the trapezoidal approximations given above are strictly correct only if the integrands go to zero at the end points. Though the X's & Y's have been constrained to go to zero at their end points the integrands represented in eqtns. (57) in fact do not. Thus knowledge of the end point values of the integrands is required and since this is not forthcoming from the equations, we usually take a Taylor expansion about a known point to get a first order approximation to the end point values. Such a procedure has the effect of adjusting the coefficients of the extreme Y_k's & X_k's in eqtns. (57) but since this would cloud the presentation unnecessarily it is here omitted.

The boundary conditions (52) become finally,

$$X_o = X_N = 0 \ ,$$

and

$$Y_o = Y_N = 0 \qquad (58)$$

giving the whole finite difference system 2N+4 equations

in as many unknowns. The solution of the system is started by substituting eqtns. (58) into eqtns. (56) and the corresponding equations in the Y's, for $k = 1$ and $k = N-1$. This eliminates the unknowns X_o, X_N, Y_o & Y_N and reduces the order of the system of unknowns and equations to 2N.

Before introducing a Newton-Raphson algorithm for solving the system, it is most convenient to alter the notation slightly. It is desirable to think of all the unknowns, the X_k, Y_k, E and A on equal footing. With this goal in mind we make the following definitions,

$$X_{k+N-1} = Y_k \ , \qquad k = 1, \ n - 1, \tag{59}$$

$$X_{2N-1} = A \ ,$$

$$X_{2N} = E \ . \tag{60}$$

We note in passing that the definition (59) ($k = 1$) has nothing whatsoever to do with the boundary condition (58). X_N (of (58)) has been discarded from the list of unknowns and we are merely reusing the symbol in place of Y_1.

Now that we have all the unknowns notationally on the same footing, we simply number the equations 1 to 2N, first taking (56) ($k = 1, \ldots, N-1$), then the corresponding Y eqtns. ($k = 1, \ldots, N-1$) and finally (57a) and (57b). In the revised notation this system

can be represented formally as

$$f_k(X_1 X_2 \ \ldots \ X_{2N}) = 0 \qquad k = 1, \ \ldots \ , \ 2N, \tag{61}$$

where each f_k corresponds to one of the above mentioned equations.

The equations (61) are a set of nonlinear algebraic equations, and, starting with an initial guessed solution, can be solved by means of a generalized Newton-Raphson iterative method (Ref. 24). Let $\bar{X}^{(n)} = (X_1^{(n)}, \ \ldots \ X_{2N}^{(n)})$ be a vector whose components are the values of the unknowns in (61) at the n^{th} iteration, and also define $\bar{F}^{(n)} = (f_1(\bar{X}^{(n)}), \ \ldots \ f_{2N}(\bar{X}^{(n)}))$. Then at the $(n+1)^{th}$ iteration the solution vector is given in terms of values at the n^{th} iteration by,

$$\bar{X}^{(n+1)} = \bar{X}^{(n)} - (J^{(n)})^{-1} \ \bar{F}^{(n)} \ , \tag{62}$$

where J is a Jacobian matrix, the elements of which are,

$$J_{\ell m}^{(n)} = \left(\frac{\partial f_\ell}{\partial X_m} \right)^{(n)} \tag{63}$$

The iteration (62) is repeated until

$$\max(|f_1(\bar{X}^{(n)})|, \ \ldots \ , |f_{2N}(\bar{X}^{(n)})|) \leq \text{tolerance}, \tag{64}$$

since when $\bar{F}^{(n)} = 0$ the system of finite-difference equations is solved exactly. A very efficient algorithm,

has been developed for the rapid solution of (62). The algorithm, which has been described in a previous paper Ref. (24), is based on the sparse and near-tridiagonal properties of the Jacobian matrix.

It remains to determine a starting vector $X^{(0)}$ for the algorithm. We have found that the procedure will easily converge from the poorest of starting solutions but probably the simplest to generate and apply are united atom wavefunctions. Once a solution has been obtained for one value of R it is a simple matter to use that solution as a starting solution for another nearby value of R. In this way it is possible to quickly obtain the wavefunctions for many values of R.

In these calculations the mesh point distribution has quite a bearing on the accuracy of the final result and we have found that the distribution should emphasise that region of the wavefunction which has the greatest contribution. This emphasis is obtained by varying the constants A & C in the coordinate transformations (49). The operators required for integral calculations in eqtns. (9) are given in confocal elliptic coordinates by,

$$\frac{d\psi}{dR} = \frac{\partial L}{\partial \lambda}\frac{\lambda(1-\lambda^2)}{(\lambda^2-\mu^2)} M + L\frac{\mu(\mu^2-1)}{(\lambda^2-\mu^2)}\frac{\partial M}{\partial \mu} + \frac{\partial L}{\partial R} M + L \frac{\partial M}{\partial R} , \qquad (65)$$

where $\psi = L(\lambda)M(\mu)$ (note that the ϕ part of ψ does not depend on R at all) and,

$$L_y = i\left[-\frac{\mu\sqrt{(\lambda^2-1)(1-\mu^2)}}{(\lambda^2-\mu^2)}\cos\phi\,\frac{\partial}{\partial\lambda} + \frac{\lambda\sqrt{(\lambda^2-1)(1-\mu^2)}}{(\lambda^2-\mu^2)}\,x\right.$$

$$\left.\cos\phi\,\frac{\partial}{\partial\mu} + \frac{\lambda\mu}{\sqrt{(\lambda^2-1)(1-\mu^2)}}\sin\phi\,\frac{\partial}{\partial\phi}\right]. \qquad (66)$$

Some of the above operators involve derivatives of the wavefunction with respect to the internuclear separation R. These are calculated numerically by evaluating the wavefunction at R and then at R + ΔR leading to a computation of the derivative using eqtn. (55a). All integrals are computed using the trapezoidal approximation including any end-point corrections which may be necessary.

One can improve the accuracy by taking more mesh points, but roundoff error increases with the number of mesh points. Instead we make an extrapolation to the $h_1 = h_2 = 0$ limit based on a number of calculations at different finite sizes of h_1 & h_2. This technique is known as the Richardson extrapolation procedure (Ref. 28). Let Q be a quantity like the electronic energy E, separation constant A or matrix element of some operator which depends on a finite difference solution. Then, if h_1 is a function of h_2, the procedure assumes that Q is a continuous function of the mesh spacing h_1 and Q is expanded in a Taylor Series about the point $h_1 = 0$. However, since inverting the coordinate system, corresponding to $h_1 \to -h_1$, cannot change the resulting value of Q, we can omit all terms containing odd powers of h_1.

Thus,

$$Q = a_1 + a_2 h_1^2 + a_3 h_1^4 + \ldots , \qquad (67)$$

where a_1 is the $h_1 \to 0$ limit of Q, and hence given the Q's corresponding to several different h_1's it is possible to get a_1 to a high degree of accuracy. Results of such extrapolations may be seen in Refs. (24, 25).

In computing the present basis set three different mesh spacings have been used corresponding to N-1 = 120, 140, 160 and the eight basis functions required (37) were obtained at 66 different internuclear separations from .05 A.U. to 40 A.U.. At each of these internuclear separations all electronic energies and integrals were computed using the three different mesh spacings and all quantities were extrapolated according to eqtn. (67). During the calculation of the time evolution of the electronic wavefunction, values of the various integrals and electronic energies are required at intermediate values of the internuclear separation R, and to fill these gaps least square fit polynomials as functions of R were calculated for each of the energies & integrals. The values drawn from the resultant polynomials are never in error by more than $1:10^4$. Much of this work may be seen graphically represented in Appendix (II).

SECTION V

PRESENTATION AND DISCUSSION OF RESULTS

The main point of this work is to present and justify the Self Consistent Trajectory method of describing the nuclear motion in Proton on Hydrogen collisions of low energy and moderate to large scattering angles. Unfortunately there is very little experimental information in this region and in fact the lowest energy results of Helbig & Everhart (Ref. 1) have very large angular resolution errors associated with them. Consequently three identical calculations of charge exchange probability in the range $10^{o} < \theta < 18^{o}$ for an energy of 151 e.v. have been carried out using eqtns. (9, 34, 37). The only difference between the calculations is in the treatment of the nuclear motion which, in this range of E & θ, is the essential difference between the I.P.A. inherent in the work of McCarroll & Piacentini (Ref. 29), the common trajectory technique of Gaussorgues et. al. (Ref. 18) and the self consistent trajectory (S.C.T.) technique presented here. Thus the electronic wavefunction (described by three states $1S\sigma g$, $2p\sigma\mu$ & $2p\pi\mu$) was solved in the Time Dependent formalism subject to: 1) a straight line trajectory, 2) a trajectory determined only by the nuclear-nuclear repulsive forces, and 3) a self-consistent trajectory. The results are presented in Fig. I. The differences between the various approaches

are quite apparent and the only valid comparison that may be drawn is between the $2p\pi\mu$ probability amplitudes obtained from 2) & 3) which are approaching each other as ρ diminishes. This is as expected since the forces giving rise to the S.C.T. are largely nuclear-nuclear for very small ρ. The results of Fig. I, along with similar results published in the paper of Gaussorgues et. al (Ref. 18), serve to illustrate the fact that, at low energies and moderate to large scattering angles, a time-dependent potential is required to describe the nuclear motion.

Another interesting result of this research is presented in Fig. II and shows the effect of the inclusion of higher states in the basis set. It was found that at an energy of 1kev the radial excitation of the gerard states $2s\sigma g$ & $3D\sigma g$ had a significant effect on the probability of charge exchange curve. S.C.T. calculations using three state, five state and seven state (as in Fig. II) expansions were carried out and they show that higher states do have an important contribution at an energy of 1 kev. In the range of scattering angle studied closer agreement between the three state S.C.T. calculation and the three state calculation of Gaussorgues et. al. should have been obtained and the discrepancy is unaccounted for. However, the seven state calculation is in excellent accord with experiment, with the probability of exchange curve having slightly higher values than the experimental points for $\theta > 4^{o}$, as would be expected

due to the experimental angular resolution errors involved. In preliminary investigations I found that the states $3S\sigma g$, $4f\sigma u$ were barely excited through radial interactions in collisions of up to 1 kev and this led to the final basis set as noted in eqtns. (37).

Typical low energy (151, 250 e.v.) results are given in Figs. III & IV (prob. of charge exchange v scattering angle) and in Figs. VII & VIII (reduced DSCS's v scattering angle), however the experimental data does not extend to large enough scattering angles for comparison to be made. Good agreement with the results of McCarroll et. al. (Ref. 29) is obtained, even at very small scattering angles. But this small angle accuracy is not experienced in inelastic calculations using the S.C.T. method.

Fig. IX shows the reduced DSCS's obtained for an incident energy of 700 e.v., where the discrepancy between this work and that of Gausscrgues et. al. (Ref. 18) in describing the small angle behaviour of the reduced DSCS for direct or exchange scattering into the $2p\pm1$ state, should be noted. This error is due to the single classical trajectory assumption inherent in the S.C.T. method. The Proton on Hydrogen collision problem, including inelastic processes is a multichannel problem and the use of the S.C.T. method is equivalent to forcing each of these channels along a common trajectory. However the single trajectory approximation becomes more acceptable for larger energies and larger scattering angles

where the trajectories associated with each channel approach the self-consistent trajectory. Thus the single trajectory assumption creates a lower limit for the applicability of the S.C.T. method which is about $E\theta \approx 1400$ e.v. deg. In Figs. (VII - X) the limiting points where the inelastic DSCS's predicted in this work become inaccurate are marked by a vertical slashed line. This lower limit applies to inelastic calculations only whereas the elastic phases (which lead mainly to the charge exchange probability curves) are predicted quite accurately for all θ justifying further the approximation of eqtn. (21).

Some higher energy (700 e.v., 1000 e.v.) seven state calculations are presented in Figs. V & VI and the discrepancies between this work and that of Gaussorgues has been shown to be due to the inadequacy of their basis set. It should be noted that the experimental points given in Fig. IX are scaled to the results of Gaussorgues et. al. (Ref. 18) and not to the results of this work. Scaling in such logarithmic presentations would result in all of the experimental points being displaced by the same amount. The results of Chidichimo-Frank & Piacentini Ref. (13) were calculated using the Eikonal approximation developed by McCarroll & Salin Ref. (11) and a five state molecular expansion ($1S\sigma g$, $2p\sigma\mu$, $2p\pi\mu$, $3p\sigma\mu$, $3p\pi\mu$) coupled using exact matrix elements of $\langle\mu_m|L_y|\mu_n\rangle$ (see eqtn. 9). Some of their results are reproduced in Fig. X along with inelastic results calculated by Gaussorgues & Salin

using an atomic expansion and the above mentioned Eikonal approximation.

Before elaborating further on Fig. X some difficulties associated with the higher energy studies of this work are discussed. In solutions of equations such as the Time-Dependent Schrodinger equation, it is obvious that any numerical integration may be terminated only when the result obtained is tending toward some limit. The integration in this work (see App. I) was taken to 20 A.U. and, when using a three state expansion, convergence was easily obtained within this limit. However it was found that when higher states were included such convergence could never be reached, and the higher state coefficients continued to vary. This very point is noted by Rosenthal (Ref. 14) who attributes these variations to the physically spurious limits (for large R) of the matrix elements of eqtn. 9. (see App. II for matrix elements). Essentially, the coupling introduced by the radial matrix elements does not go to zero as $R \to \infty$, and this effect gives rise to problems in calculating higher state excitation probabilities in this work. These problems are eliminated in Bate's and McCarroll's work (Ref. 3) with the introduction of other difficulties.

However, despite this problem, after integration to 20 A.U. the $1S\sigma g$, $2p\sigma\mu$, $2p\pi\mu$ state occupancies did not vary by more than 1%, while the $3p\sigma\mu$ state occupancy varied about a mean by around 20%, and consequently these results are presented in Fig. X with appropriate error bars.

(Note here that though the 2S hydrogenic state is strictly formed as a linear combination of the 2Sσg & 3pσμ molecular states, the occupancy of the 2Sσg state in these calculations, apart from the fact that it varied greatly at "convergence", is so small that it does not affect the result presented for scattering into the 2S state of Hydrogen (beyond the error bars). Consequently this work's predictions of the direct & exchange DSCS's for scattering into the 2S state, are equal).

This work's agreement with the DSCS for direct scattering into the 2S state of Hydrogen as calculated by Gaussorgues & Salin (Ref. 15) is apparent (Fig. X).

The basic theoretical difference between the work of Gaussorgues & Salin and that of Chidichimo-Frank & Piacentini (Ref. 13) is that Gaussorgues et. al. have included radial coupling elements in their calculations. One major reason for this work's agreement with that of Gaussorgues et. al. is that radial coupling elements have been included here.

It therefore appears that the neglect of velocity dependent translation factors and radial coupling elements is a mistake and that best results will be obtained by using a reasonably large basis set and translation factors. In this work it has been shown that the use of a large basis set and radial coupling elements has led to improved agreement with experiment and it is an obvious extrapolation of this result to state that near perfect agreement could be obtained with a very large

basis set. However the inclusion of translation factors would give equivalent agreement when coupled with a much smaller basis set because of the consequent elimination of convergence problems.

In this work it appears that the major effect of the inclusion of the 2Sσg & 3Dσg states is to slightly alter the classical phase of the 1Sσg state (specified by both its coefficient, a_1 (eqtn. 2.) and η_1 (eqtn. 15)) by coupling through the radial elements. This coupling is what leads, in the main, to the final agreement with experiment.

As a partial check on the accuracy of these calculations, it is interesting to note that the numerical value of the DSCS's obtained in this work agree with those of Gaussorgues et. al (Ref. 18) and hence no scaling factor was required for Fig. IX. Because of this agreement all other theoretical & experimental values have been normalized to this work's results (except in Fig. IX) at a point where the two approaches could be expected to concur.

FIGURE I

The curves A represent probability of charge exchange v impact parameter ρ using;

———— straight line trajectory approx. (I.P.A.),

------- 1/R nuclear-nuclear forces only to determine nuclear trajectory, and,

———— the self-consistent trajectory method. All of these probabilities were computed using eqtn (37).

The curves B represent the probability of excitation of the $2p\pi\mu$ state v impact parameter ρ, where the legend noted above still applies. This probability is strictly a probability amplitude which is given by,

$$P = |a_{2p\pi\mu}|^2$$

The vertical bar in this figure is repeated on Fig. III and the bars denote the corresponding point in ρ & θ space.

FIG.I

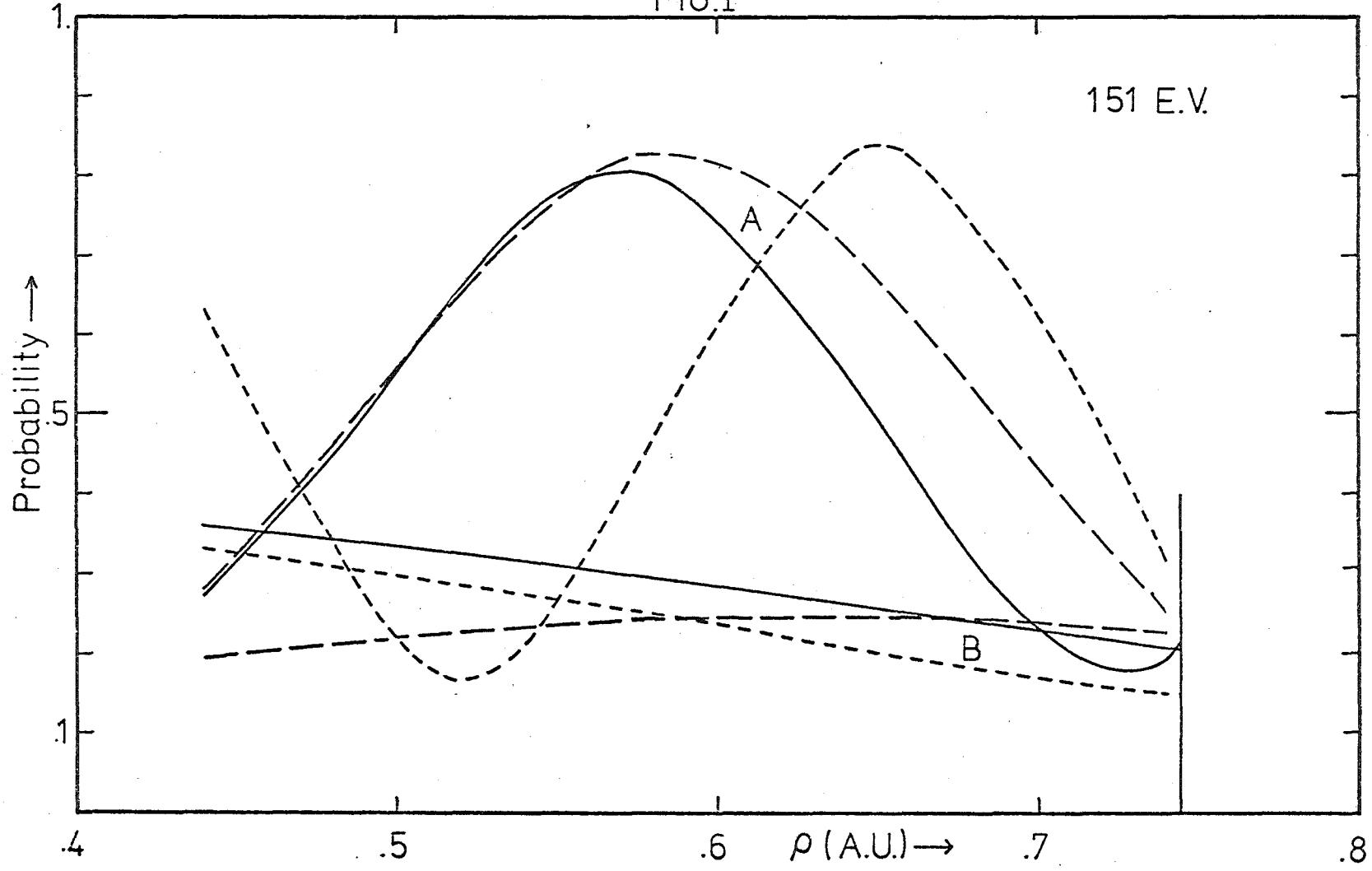

FIGURE II

All points are probability of charge exchange values v the laboratory scattering angle θ.
----- three state ($1S\sigma g$, $2p\sigma\mu$, $2p\pi\mu$) calculation of Gaussorgues et. al. (Ref. 18).

The full curves A, B, & C were all obtained using the S.C.T. method presented in this work, and they result from 3 state ($1S\sigma g$, $2p\sigma\mu$, $2p\pi\mu$), 5 state ($1S\sigma g$, $2p\sigma\mu$, $2p\pi\mu$, $3p\sigma\mu$, $3p\pi\mu$) and 7 state ($1S\sigma g$, $2p\sigma\mu$, $2p\pi\mu$, $3p\sigma\mu$, $3p\pi\mu$, $2S\sigma g$, $3D\sigma g$) calculations respectively.

The experimental points x were obtained by Houver et. al. (Ref. 2) and have an angular resolution of $.2^{o}$.

what is the assessment of this?

FIG. II

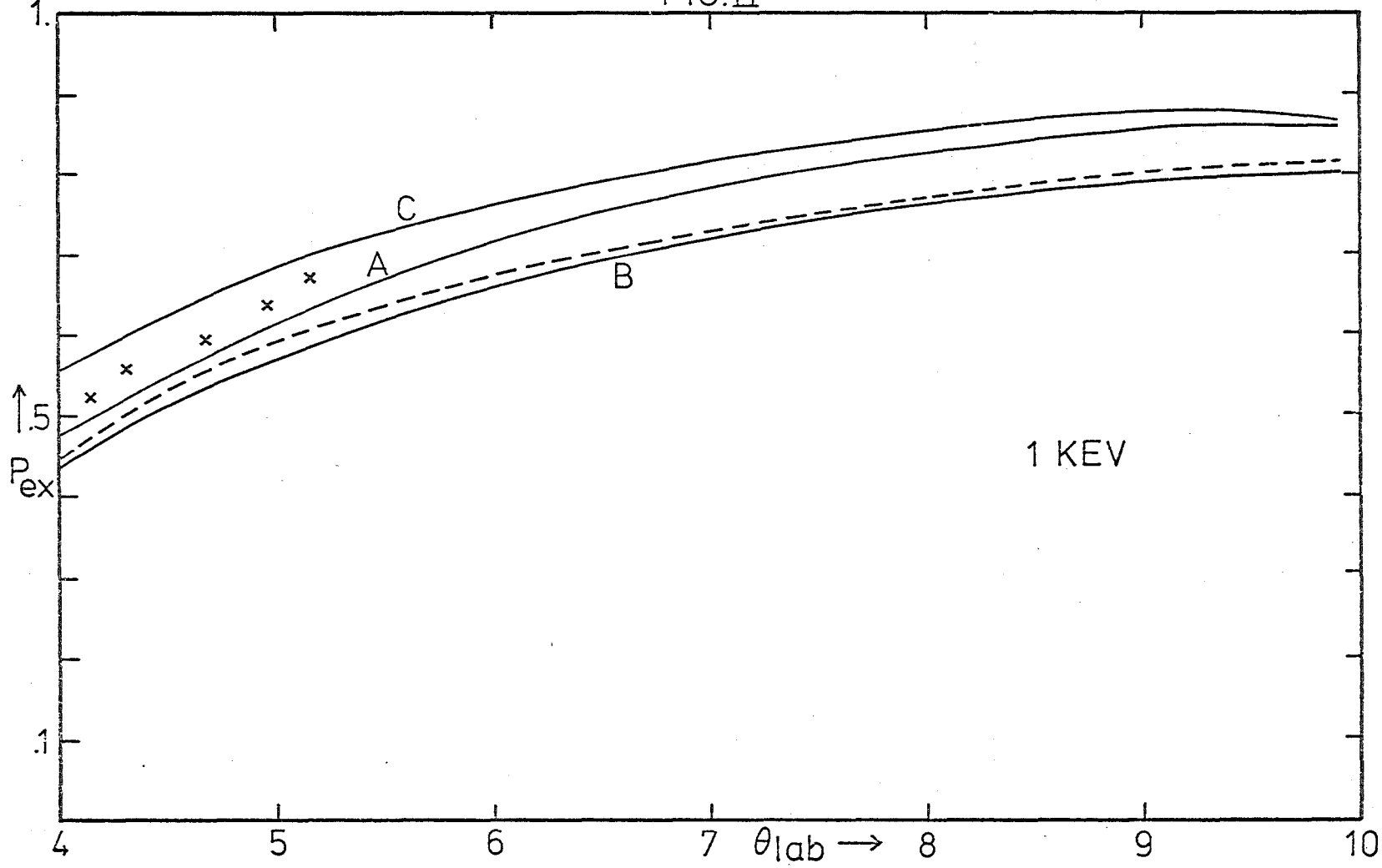

FIGURE III

Probability of charge exchange v lab scattering angle θ for incident energy E = 151 e.v..

————This work, a three state ($1S\sigma g$, $2p\sigma\mu$, $2p\sigma\mu$) calculation using the self-consistent trajectory technique.

x Experimental points of Helbig & Everhart (Ref. 1) whose angular resolutions are 1.2^{o}. The vertical bar is repeated at the same point on Fig. I to allow for comparison between figures.

FIG. III

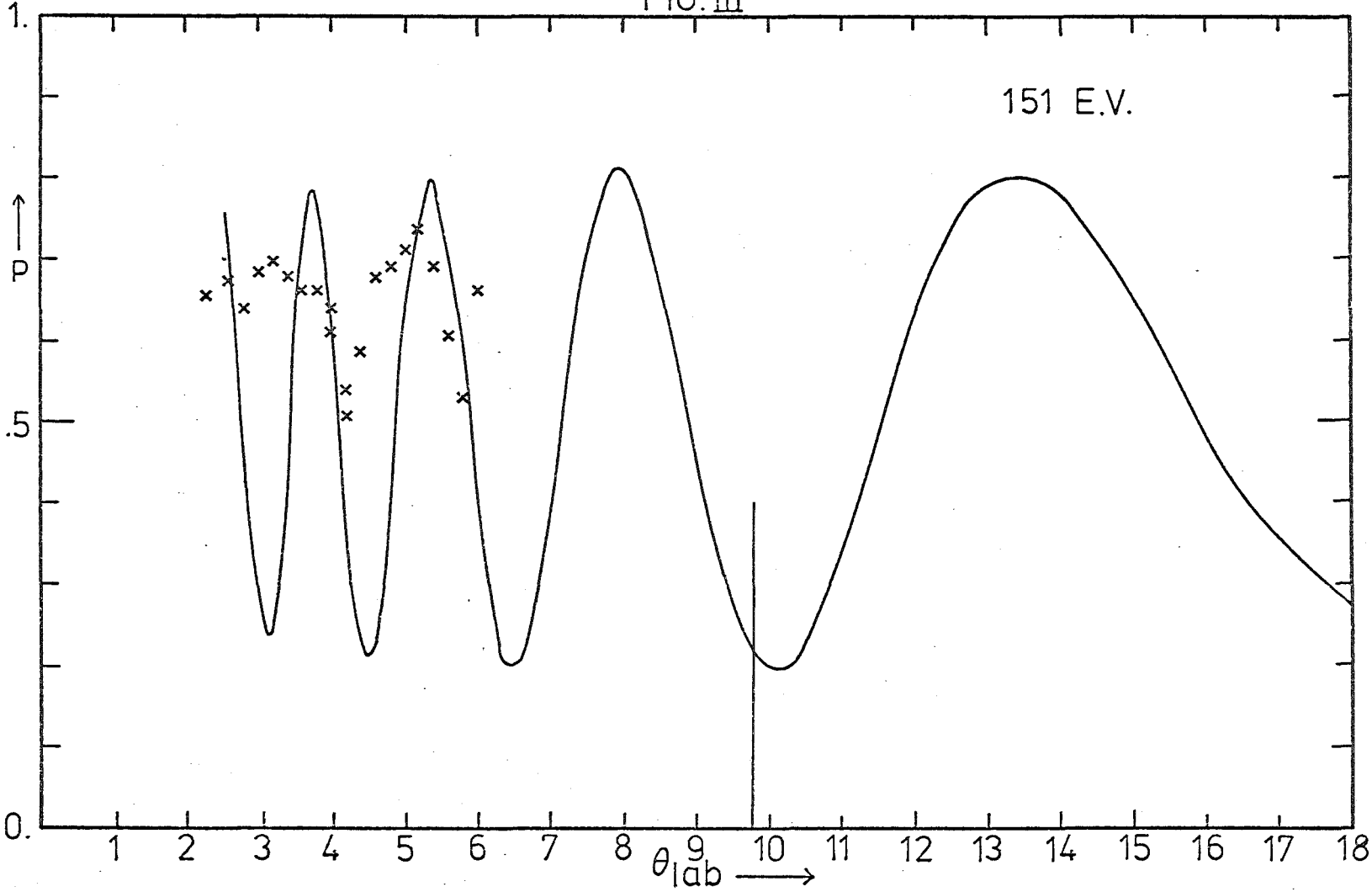

FIGURE IV

Probability of charge exchange v lab. scattering angle θ for incident energy E = 250 e.v..

------ a three state ($1s\sigma g$, $2p\sigma\mu$, $2p\pi\mu$) calculation of McCarroll et. al. (Ref. 29) using the Eikonal approximation (Ref. 11).

———— This work, also a three state calculation, using the S.C.T. technique.

x Experimental results of Houver et. al. (Ref. 2) angular resolution: $.4^{o}$.

FIG. IV

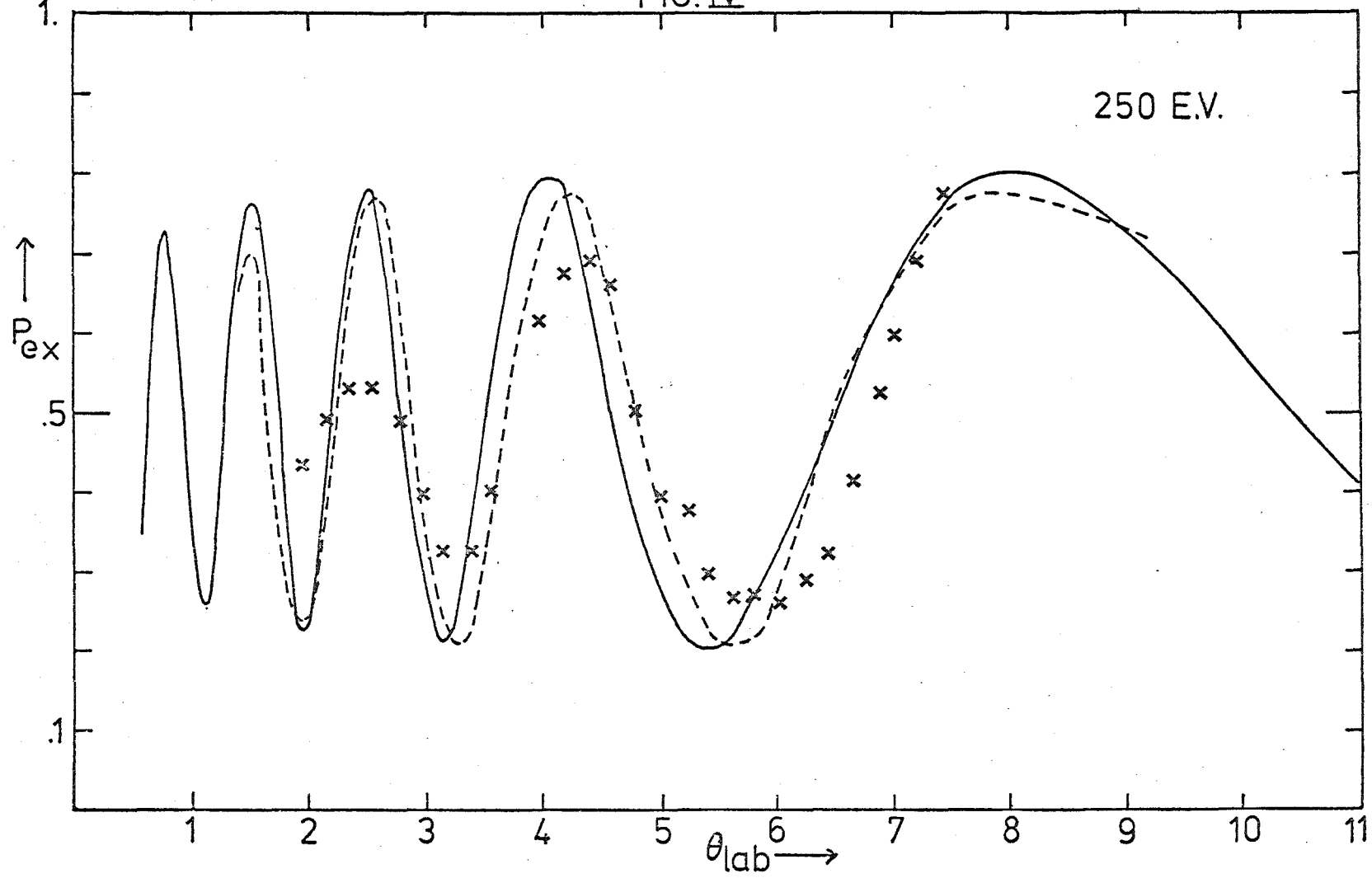

FIGURE V

Probability of charge exchange v lab. scattering angle θ for an incident energy E = 700 e.v..

------ a three state ($1S\sigma g$, $2p\sigma\mu$, $2p\pi\mu$) calculation of Gaussorgues et. al. (Ref. 18).

B This work, a seven state ($1S\sigma g$, $2p\sigma\mu$, $2p\pi\mu$, $3p\sigma\mu$, $3p\pi\mu$, $2s\sigma g$, $3D\sigma g$) calculation, using the S.C.T. technique.

A This work, a three state ($1S\sigma g$, $2p\sigma\mu$, $2p\pi\mu$) calculation, using the S.C.T. technique.

x Experimental points of Houver et. al. (Ref. 2), angular resolution = $.07^{o}$.

FIG. V

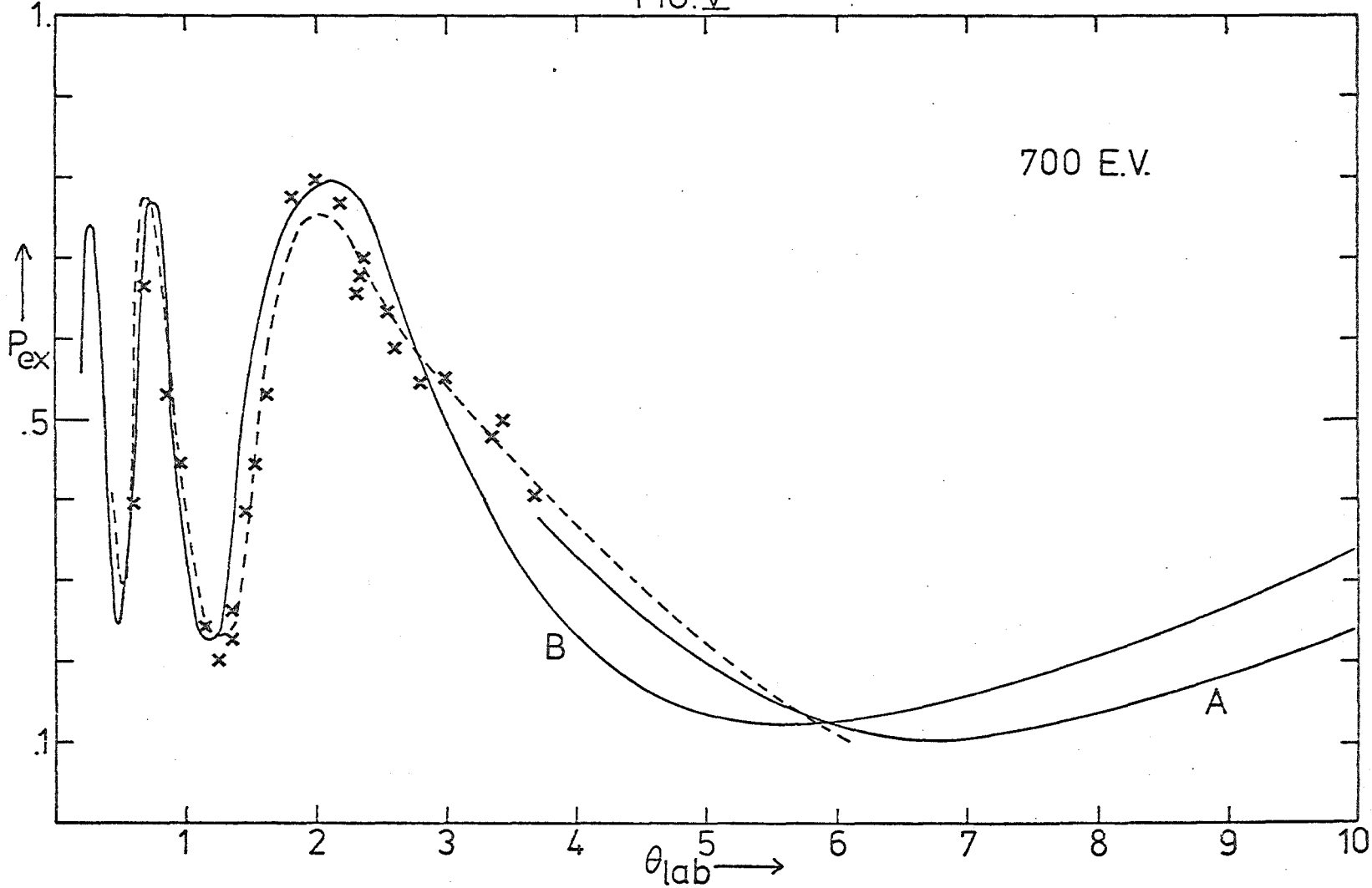

60.

FIGURE VI

Probability of charge exchange v lab. scattering angle θ for an incident energy E = 1 Kev.

------- a three state calculation ($1S\sigma g$, $2p\sigma\mu$, $2p\pi\mu$) of Gaussorgues et. al. (Ref. 18).

———— This work, a seven state ($1S\sigma g$, $2p\sigma\mu$, $2p\pi\mu$, $3p\sigma\mu$, $3p\pi\mu$, $2S\sigma g$, $3D\sigma g$) calculation, using the S.C.T. technique.

x,o Experimental results of Houver et. al. (Ref. 2)

angular resclution: x $.07^{o}$

o $.2^{o}$

FIG. VI

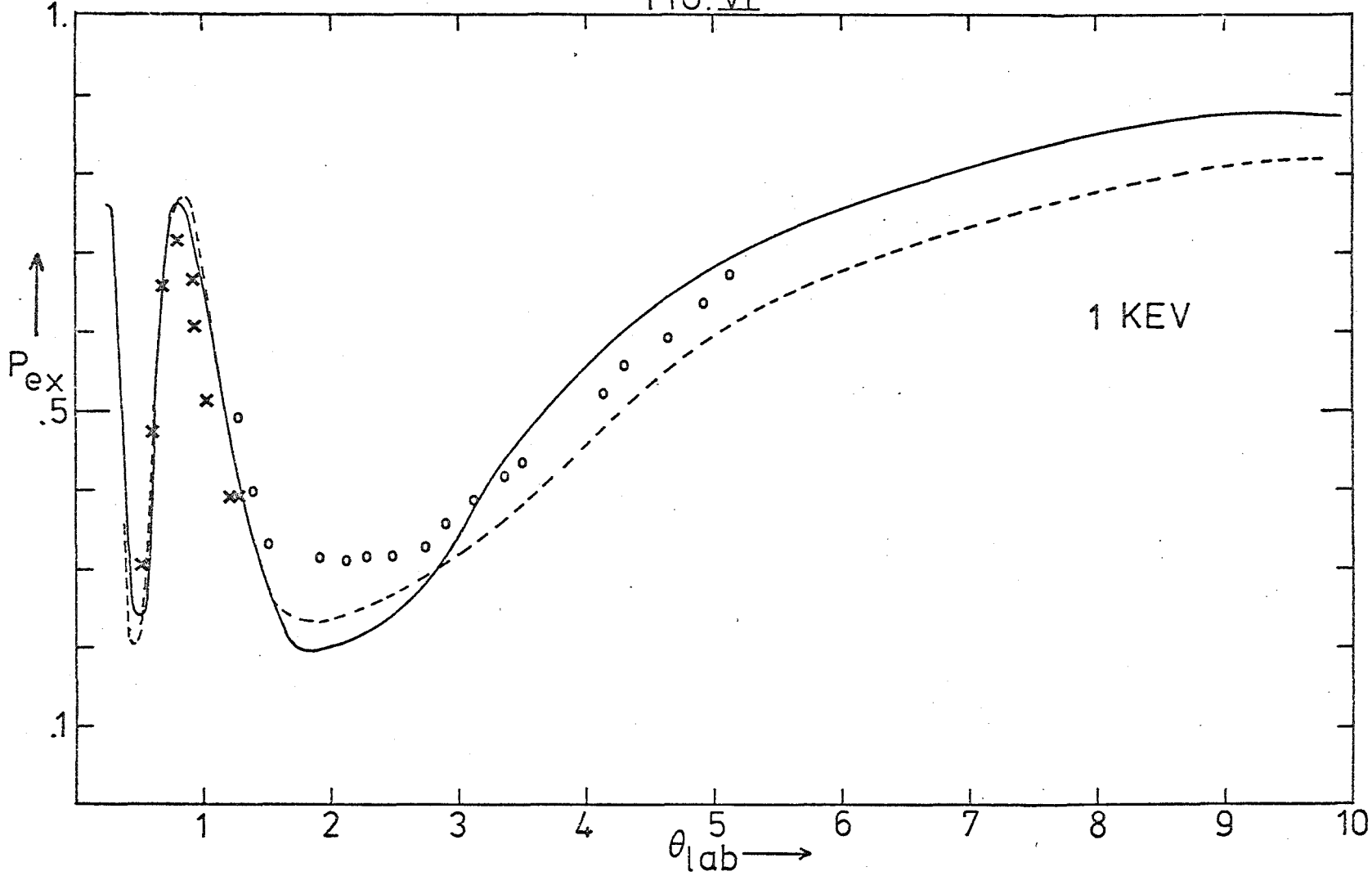

FIGURE VII

Reduced DSCS ($\theta^2 \frac{\partial\sigma}{\partial\Omega}$ degrees^2 A.U.) v lab. scattering angle θ for incident energy E = 151 e.v.. All curves are calculated for this figure as for Fig. III.

A: Total reduced DSCS for exchange,

$$\theta^2 \left(\frac{\partial\sigma}{\partial\Omega_{EX}} (1S) + \frac{\partial\sigma}{\partial\Omega_{EX}} (2p\pm1) \right) .$$

B: Reduced DSCS for direct scattering into the 1S hydrogenic state.

C: Reduced DSCS for direct or exchange inelastic scattering into the 2p±1 hydrogenic state.

FIG. VII

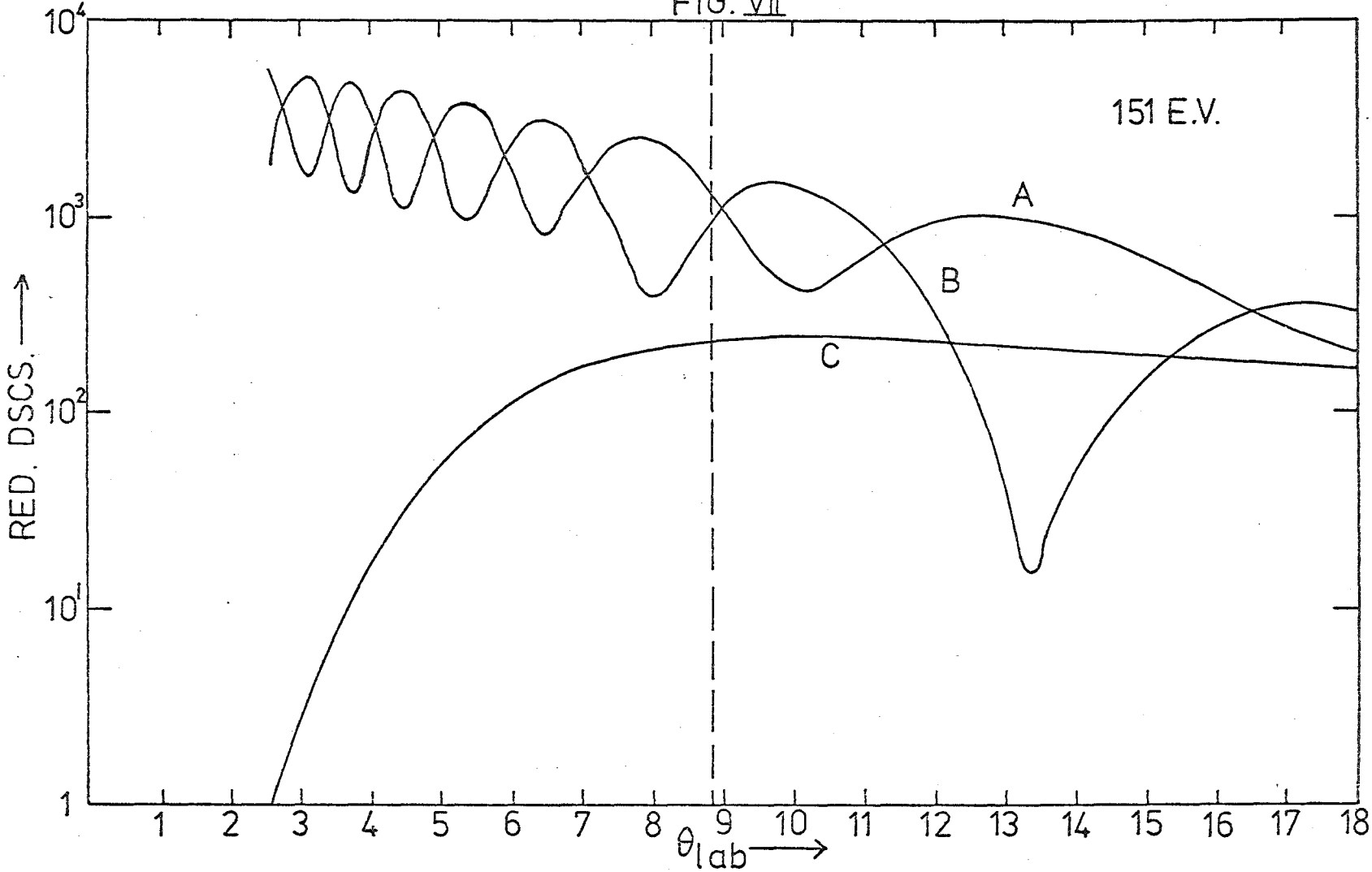
151 E.V.
A
B
C
RED. DSCS. ⟶
10^4
10^3
10^2
10^1
1
1 2 3 4 5 6 7 8 9 10 11 12 13 14 15 16 17 18
θ_{lab} ⟶

FIGURE VIII

Reduced DSCS's v lab. scattering angle θ for an incident energy E = 250 e.v..

– – – – – – Work due to McCarroll et. al. (Ref. 29).

———— This work.

x,o Experimental results of Houver et. al. (Ref. 2).

For other details see the legend of Fig. IV. The curves A, B & C have the same labelling as in Fig. VII.

FIG. VIII

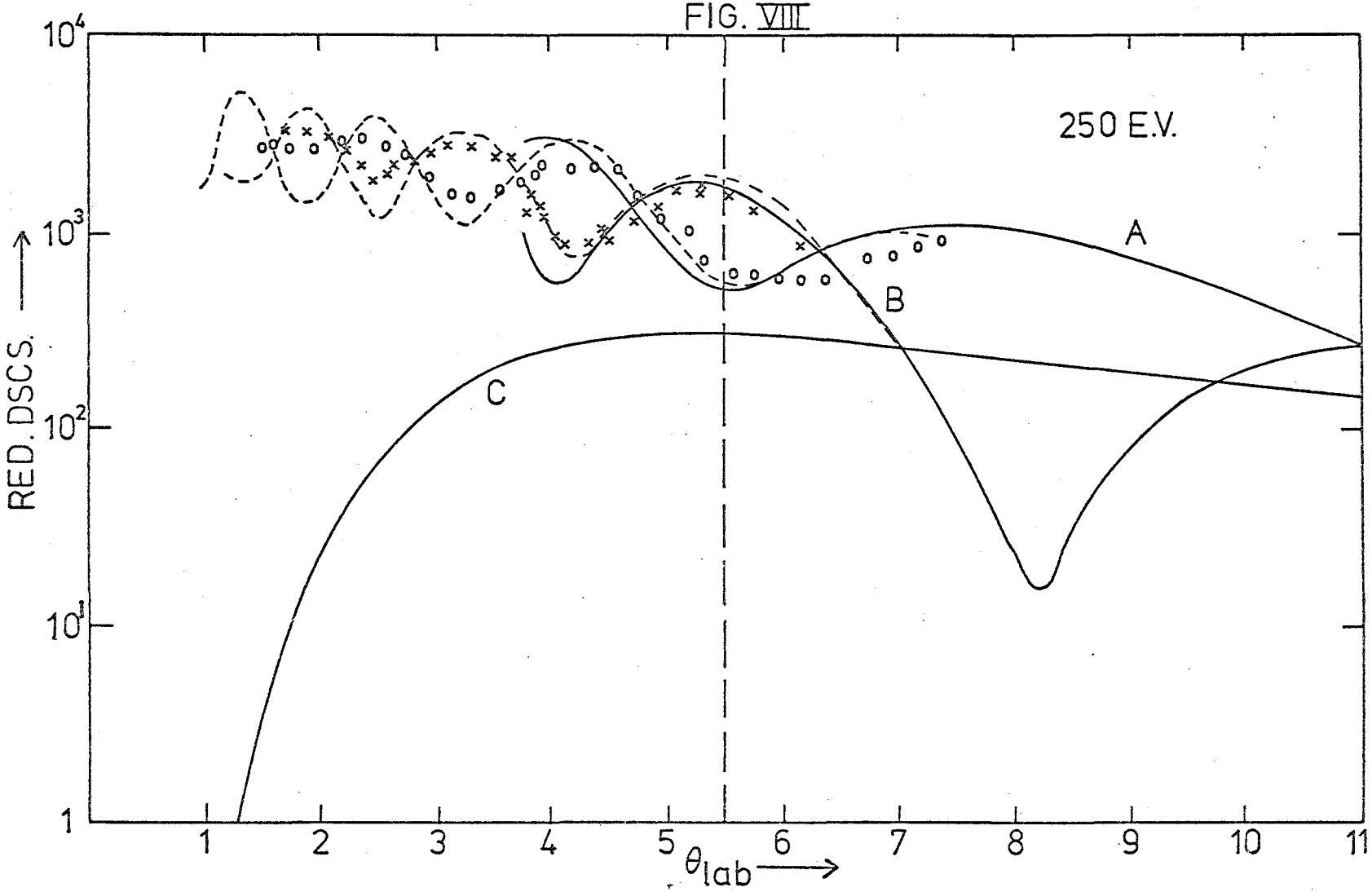

FIGURE IX

Reduced DSCS's v lab. scattering angle θ for an incident energy E = 700 e.v..

------ Work due to Gaussorgues et. al. (Ref. 18).

———— This work (seven states).

●,o,x Experimental work of Houver et. al. (Ref. 2).

For other details see the legend of Fig V. The curves A, B, & C have the same labelling as in Fig. VII. It should be noted that three state calculations (using the S.C.T. method) of the DSCS's are in closer agreement with the appropriate results of Gaussorgues et. al., but they are not presented here for the sake of clarity.

FIG. IX

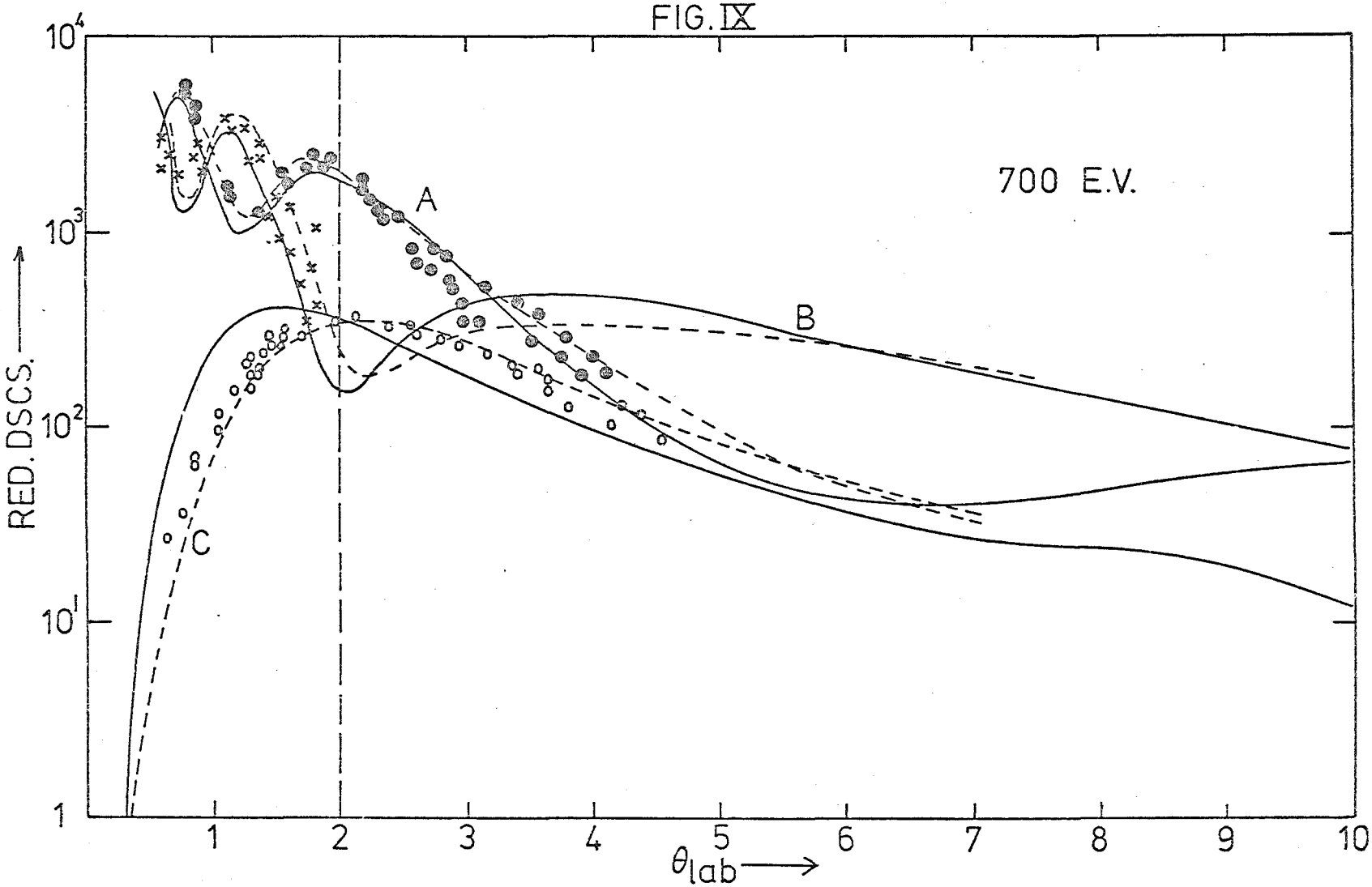

FIGURE X

DSCS's lab. scattering angle θ for an incident energy E = 1 Kev.

-------- Work of Chidichimo-Frank et. al. (Ref. 13) using a 5 state ($1S\sigma g$, $2p\sigma\mu$, $2p\pi\mu$, $3p\sigma\mu$, $3p\pi\mu$) expansion coupled with the Eikonal approx. (Ref. 11).

———————— Work of Gaussorgues & Salin (Ref. 15) using an atomic basis set and also coupled with the Eikonal approx. (Ref. 11).

———————— This work, as in Fig. VI.

x,● Experimental results of Houver et. al. The curves are all direct DSCS's and A,B & C correspond to scattering into the 1S, 2p±1 & 2S states of Hydrogen respectively.

FIG. X

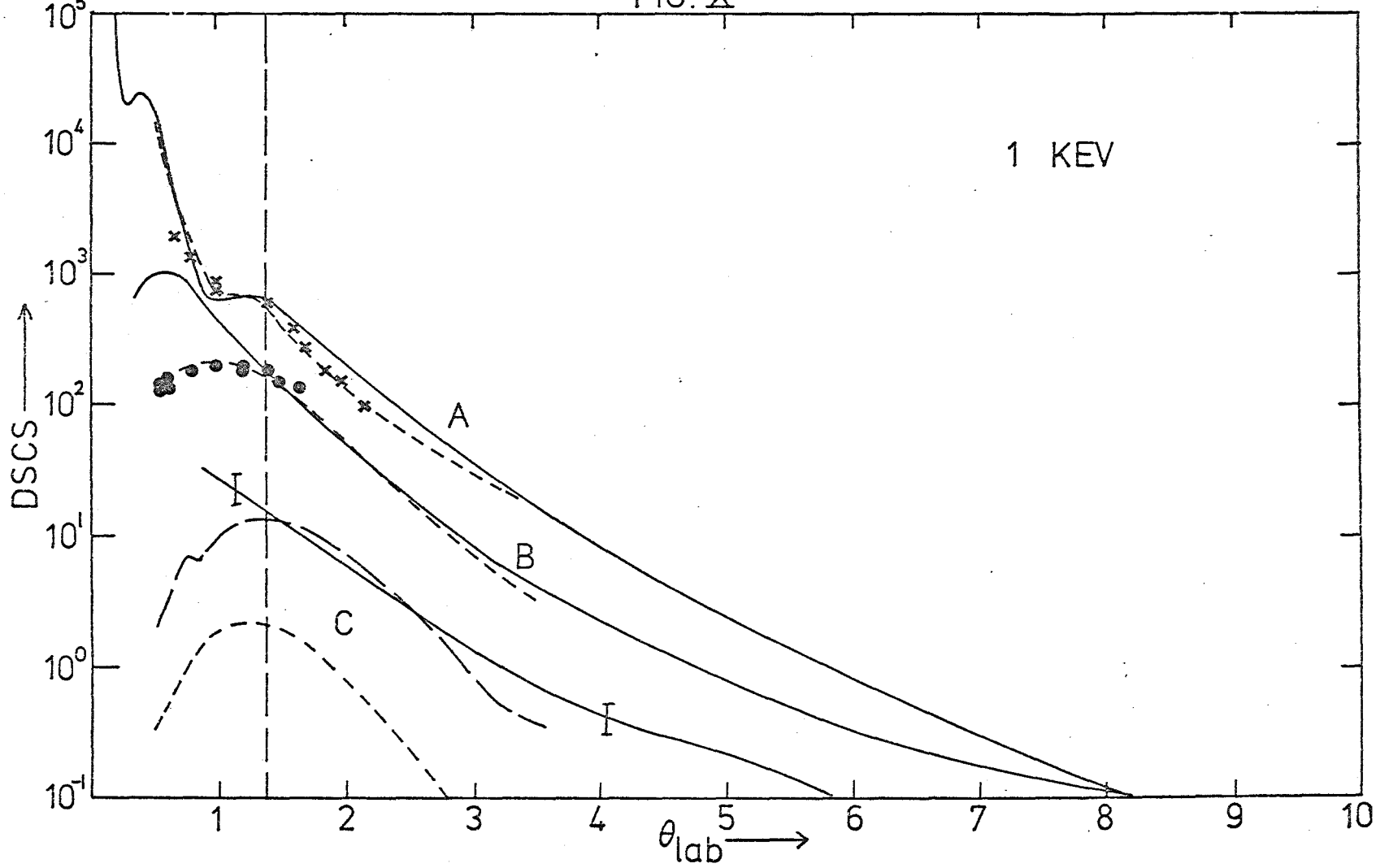
1 KEV
DSCS
θ_{lab}
A
B
C
10^5
10^4
10^3
10^2
10^1
10^0
10^{-1}
1
2
3
4
5
6
7
8
9
10

CONCLUSION

In this work it has been shown that the self-consistent trajectory method is a useful and viable method for describing small energy, large scattering angle proton on hydrogen collisions. However more experimental data is required to completely assess its accuracy.

The inclusion of higher state gerade functions in the molecular basis set has been shown to have a significant effect on the results for collision energies as low as 700 e.v.. However, the neglect of velocity dependent terms in the basis set has caused spurious excitations of some higher states which in turn leads to inaccurate inelastic cross-sections. Some effort must be made to ensure that the excitations caused by the radial coupling elements go to zero as the accelerations of the colliding nuclei go to zero.

A collegue of the writer has extended the algorithm presented in section IV to deal with single configuration H_2 (Ref. (31) and these calculations are presently being further extended to include multi-configuration and electron correlation effects. The basis functions obtained for these systems, coupled with the methods presented in this work, will enable atom-atom collisions to be accurately described.

ACKNOWLEDGEMENTS

The author wishes to express his grateful appreciation to Dr Bill Fimple whose enthusiastic assistance and advice were invaluable during the course of this work.

I would also like to thank Steve White and Martin Unwin for many useful discussions and ideas.

Gratitude is extended by the author to the Physics Department of the University of Canterbury for constant financial assistance.

APPENDIX I

COMPUTATIONAL DETAILS

The following consists of a general discussion regarding some of the more technical details involved in obtaining the results.

The basis set was evaluated at the following internuclear separations:

$R = .05 \rightarrow .5$, $\Delta R = .05$,

$R = .5 \rightarrow 2$, $\Delta R = .1$,

$R = 2 \rightarrow 5$, $\Delta R = .25$,

$R = 5 \rightarrow 10$, $\Delta R = .5$,

$R = 10 \rightarrow 20$, $\Delta R = 1$,

$R = 20 \rightarrow 40$, $\Delta R = 2$,

where A.U. are the units involved. At each of these internuclear separations the basis set was evaluated for N = 120, 140, 160, where N is the number of mesh points in each dimension of the wavefunction.

The radial and angular integrals were evaluated at each internuclear separation three times using the three different basis sets corresponding to N = 120, 140, 160, and the results were then extrapolated using the technique discussed in section IV. Accuracies for the resulting eigenenergies and integrals

ranged from 1 part in 10^5 to 1 part in 10^8.

To enable evaluation of the various integrals and eigenergies at intermediate values of the internuclear separation, some sort of interpolating procedure is required and consequently a least squares (LSQ) fit technique has been used.

If it is assumed that these quantities are continuous functions of R then it is possible to state that,

$$Y(R) = a_0 + a_1 R + a_2 R^2 + \ldots a_M R^M \quad , \tag{1}$$

to some degree of accuracy, where the a_i are unknown coefficients and where Y(R) represents an approximation to the functional dependence of an integral or eigenenergy on R. If Y_i, i = 1, N represents a set of exact solutions to Y(R) at the points R_i, i = 1, N, then the least-square criterion may be written,

$$S = \sum_{i=1}^{N} (Y_i - Y_i')^2 \quad , \tag{2}$$

where the Y_i' are given by (1) after substitution of the R_i, i = 1, N, and where S is to be minimized.

The way in which this is carried out is to differentiate (2) with respect to each of the a_i, i = 0,M, and set each differential to zero. Thus a set of M+1 equations in M+1 unknowns is obtained,

$$Na_0 + \sum R_i a_1 + \ldots \quad + \sum R_i^M a_m = \sum Y_i$$

$$\sum R_i a_o + \sum R_i^2 a_1 + \ldots \quad + \sum R_i^{M+1} a_m = \sum R_i Y_i$$

$$\ldots\ldots\ldots\ldots\ldots\ldots\ldots\ldots\ldots\ldots\ldots\ldots$$

$$\sum R_i^M a_o + \sum R_i^{M+1} a_1 + \ldots \quad + \sum R_i^{2M} a_m = \sum R_i^M Y_i \quad , \qquad (3)$$

and here $\sum$ implies $\sum_{i=1}^{N}$. These equations are simultaneous and may be solved by any standard sub-program. The accuracy of the resulting polynomial may be easily checked by resubstitution of the R_i. At no stage are polynomials of greater order than M = 10 required and the resulting accuracy is never worse than 1 part in 10^4.

Due to the variations in the integrals and eigenenergies with R, it was decided to evaluate the LSQ polynomials over discrete ranges of R. Consequently three polynomials were computed for each integral and eigenenergy, and these give accurate values in the ranges; $.05 \leqslant R \leqslant .5$, $.5 \leqslant R \leqslant 10$, $10 \leqslant R \leqslant 40$ respectively, where A.U. are used.

Graphical representations of all eigenenergies and integrals are presented in App. II along with the LSQ polynomials.

Equations (9) were integrated numerically from their starting solutions (eqtns. 5) using the standard 4^{th} order Runge-Kutta method. The integrations were taken from an internuclear separation R of about 20 A.U. (approximately ∞) out to 20 A.U., in about 1500 equally spaced time points. These parameters were varied so that

the final results obtained (excluding the higher state results as previously discussed) did not change by more than 1%. The trajectory along which the electronic wavefunction was solved, was divided into 3000 points equally spaced in time. At each of these points in space the appropriate polynomials are evaluated to give the values of the integrals and eigenergies of the contributing states. A large saving in computer time would occur if an integration technique giving emphasis to the region of closest approach was employed.

The results for each energy come from solutions of the electronic wavefunction corresponding to about 60 different values of the impact parameter ρ. These values are chosen to give the smooth curves in the Figs. (I-X).

In the calculations of the scattering amplitudes given in eqtn. (34) it is necessary to know ρ_i & $\frac{\partial \rho_i}{\partial \theta}$ as functions of the scattering angle θ, for each of the contributing electronic states ($i = 1, \ldots N$). This functional dependence is also obtained by fitting a LSQ polynomial through a number (about 50) of previously calculated points. These points are calculated by setting the initial conditions (impact parameter ρ and incident energy E), subjecting the system to a potential caused by the electronic state in question, numerically integrating to a large internuclear separation, and hence obtaining a scattering angle θ.

APPENDIX II

GRAPHICAL REPRESENTATIONS OF THE INTEGRALS AND EIGENENERGIES; THE LSQ POLYNOMIALS.

The following two figures show the variations of the radial and angular integrals as functions of R, the internuclear separation. These values are required for the solution of eqtns. (9).

The numerical values for Figs. (XI-XIII) were obtained by evaluating the LSQ polynomials presented in Tables (I-III) respectively.

To use the LSQ polynomials to evaluate any integral or eigenenergy at a particular R, the coefficient indicated by the label 1 is the constant term in the expansion, whilst the succeeding numbers labelled by 2→11 are the coefficients corresponding to powers of R 1→10 respectively.

FIGURE XI

Radial Integrals:

A, $\langle 1S\sigma g|\frac{d}{dR}|2S\sigma g\rangle$

B, $\langle 2p\pi\mu|\frac{d}{dR}|3p\pi\mu\rangle$

C, $\langle 2p\sigma\mu|\frac{d}{dR}|3p\sigma\mu\rangle$

D, $\langle 1S\sigma g|\frac{d}{dR}|3D\sigma g\rangle$

E, $\langle 2S\sigma g|\frac{d}{dR}|3D\sigma g\rangle$

Note: the above are the only non-zero radial integrals formed between the states of the maximum sized basis set mentioned previously.

FIG. XI

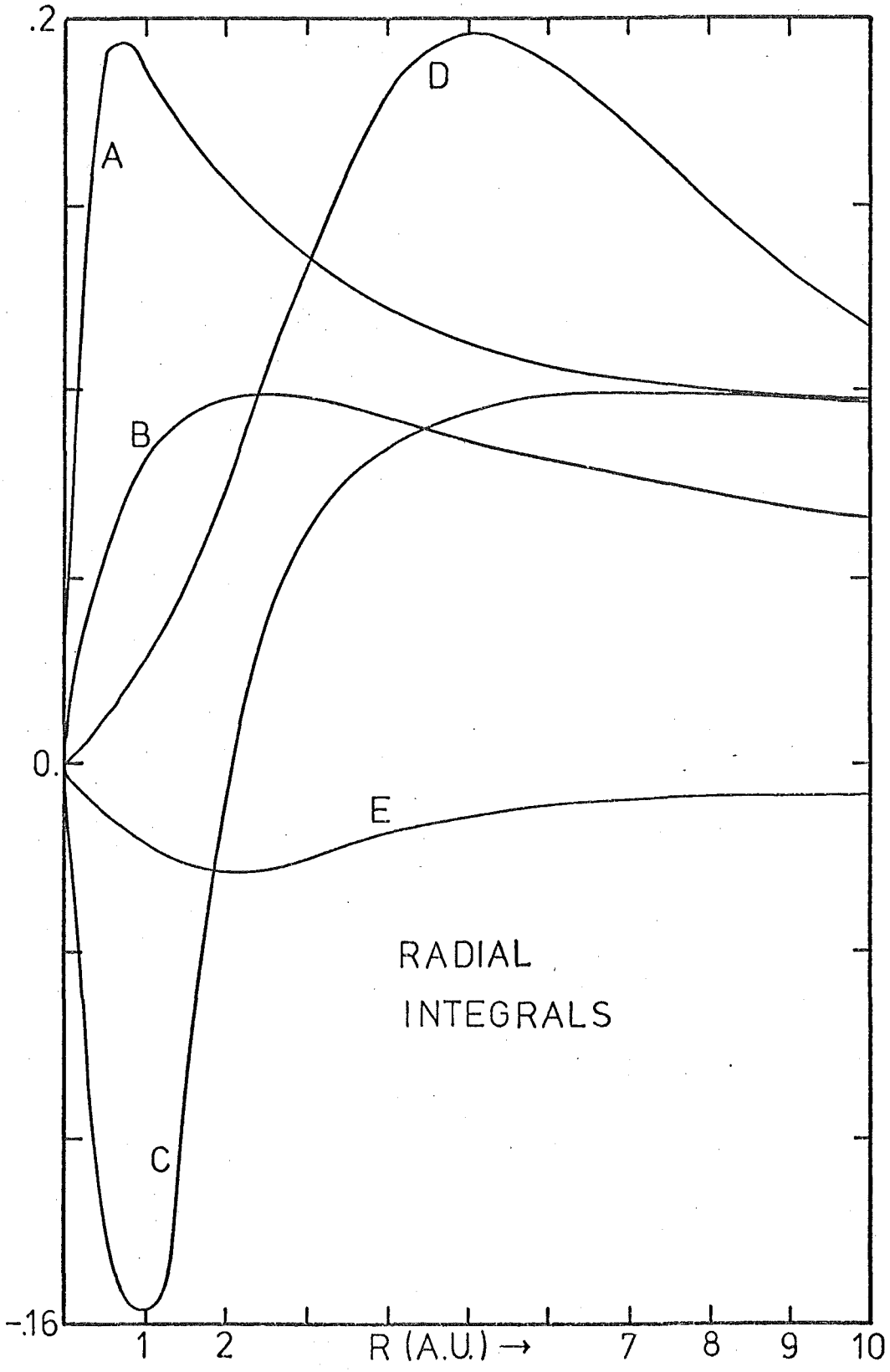

FIGURE XII

Angular Integrals:

A, $\langle 2p\pi\mu|Ly|2p\sigma\mu\rangle$

B, $\langle 3p\pi\mu|Ly|2p\sigma\mu\rangle$

C, $\langle 1S\sigma g|Ly|3D\pi g\rangle$

D, $\langle 2S\sigma g|Ly|3D\pi g\rangle$

E, $\langle 2p\pi\mu|Ly|3p\sigma\mu\rangle$

F, $\langle 3p\pi\mu|Ly|3p\sigma\mu\rangle$

G, $\langle 3D\pi g|Ly|3D\sigma g\rangle$

Note: the above are the only non-zero angular integrals formed between the states of the maximum sized basis set mentioned previously.

FIG. XII

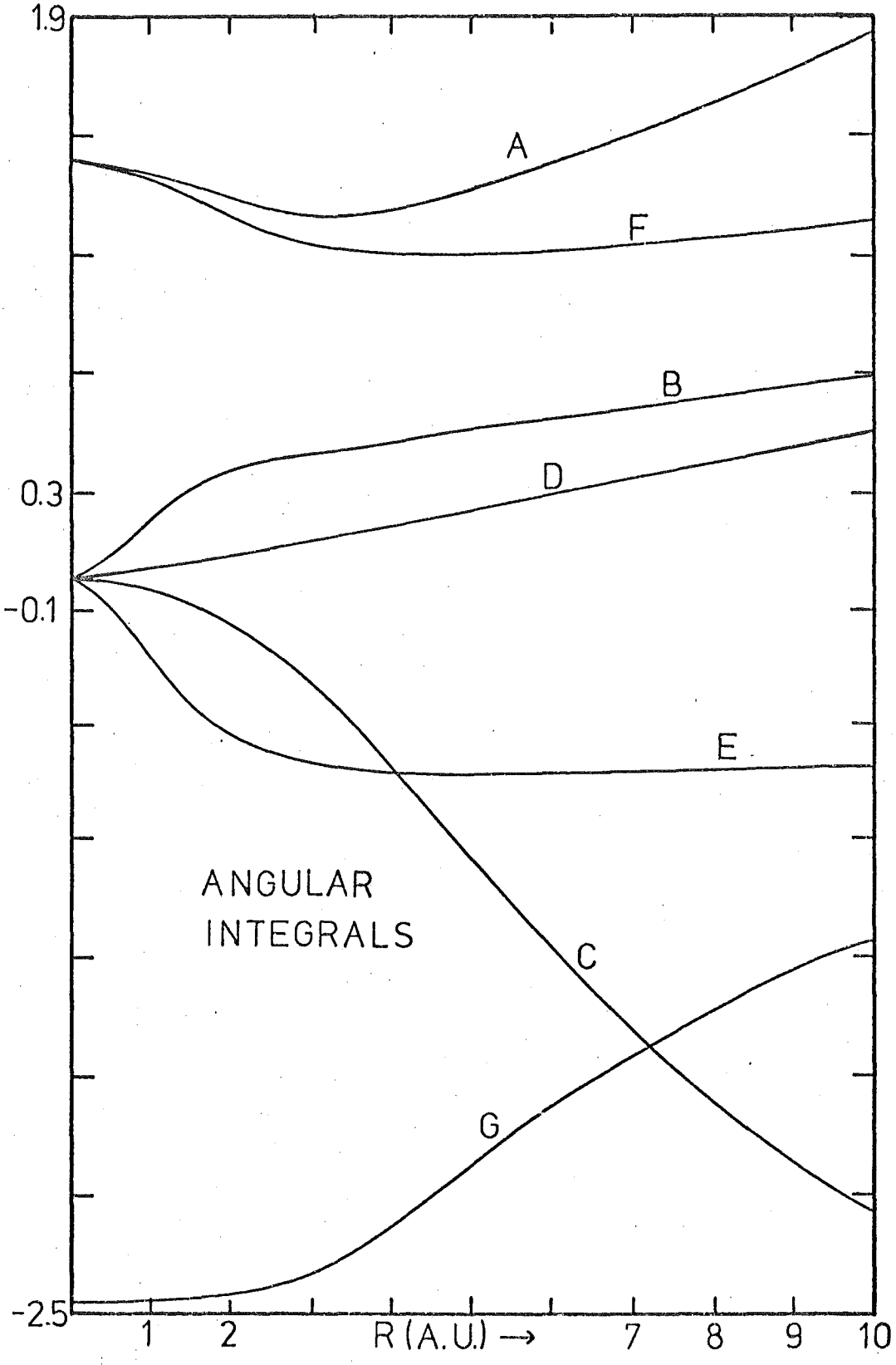

FIGURE XIII

H_2^+ energy eigenvalues:

(Only the electronic energy is graphed.)

A, 1Sσg

B, 2pπμ

C, 2Sσg

D, 3pπμ

E, 2pσμ

F, 3Dπg

G, 3pσμ

H, 3Dσg

FIG. XIII

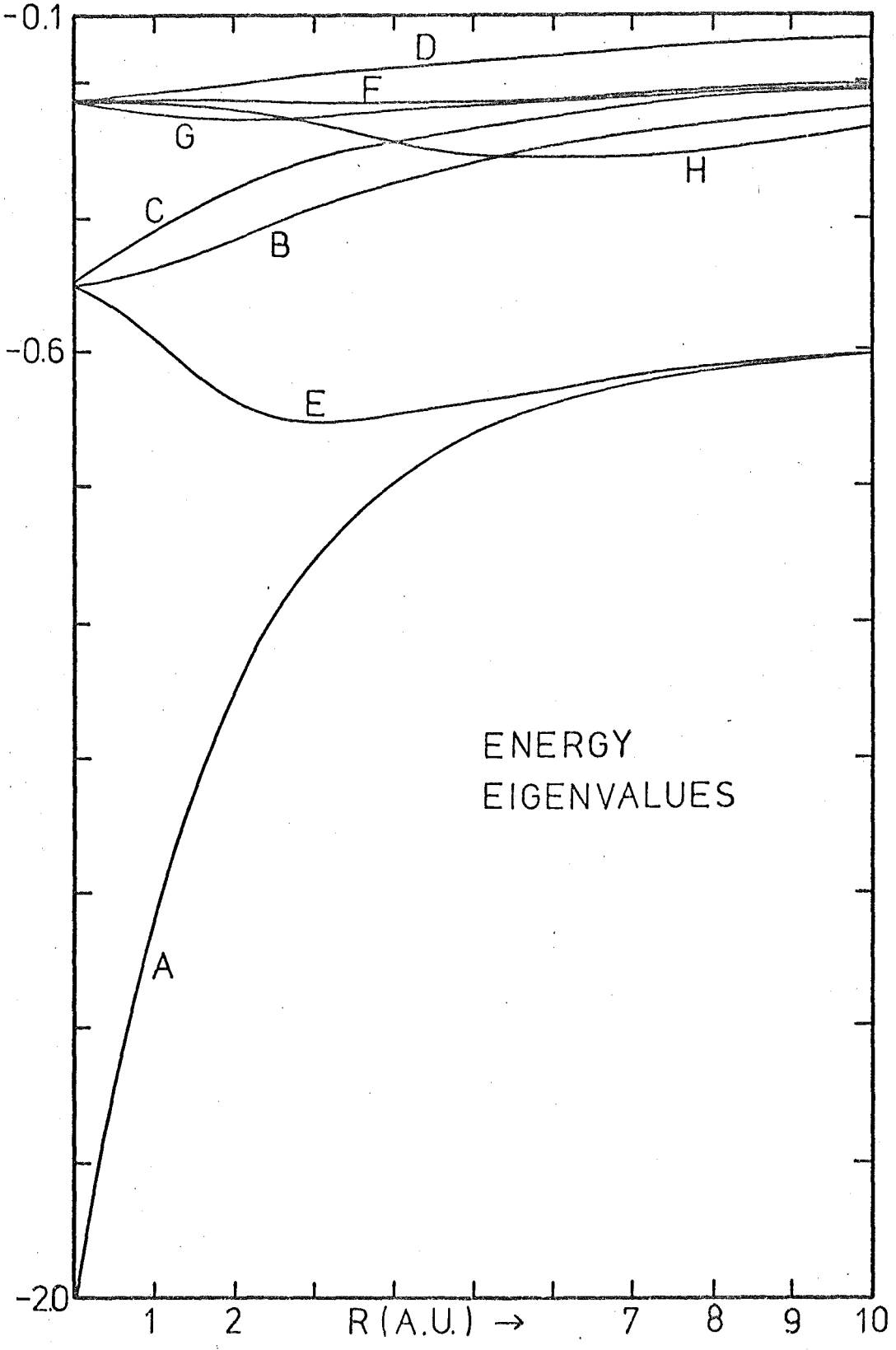

TABLE I

	A	B	C	D	E
	INTERNUCLEAR SEPARATION R=10.00 A.U. TO 40.00 A.U.				
1	.306229E+00	.226487E+00	.469931E-01	.115434E+01	.154488E+00
2	-.857793E-01	-.582943E-01	.245987E-01	-.366973E+00	-.796910E-01
3	.156400E-01	.103477E-01	-.483598E-02	.609496E-01	.159348E-01
4	-.167335E-02	-.113789E-02	.532343E-03	-.623615E-02	-.177483E-02
5	.116217E-03	.803003E-04	-.372392E-04	.418326E-03	.125421E-03
6	-.547608E-05	-.372160E-05	.174902E-05	-.197439E-04	-.594838E-05
7	.177270E-06	.114180E-06	-.561497E-07	.556319E-06	.192903E-06
8	-.339245E-08	-.228945E-08	.121907E-08	-.106765E-07	-.423641E-08
9	.554788E-10	.286851E-10	-.171802E-10	.124841E-09	.603853E-10
10	-.463479E-12	-.201976E-12	.141946E-12	-.779778E-12	-.504796E-12
11	.172351E-14	.600949E-15	-.521990E-15	.183215E-14	.187988E-14
	INTERNUCLEAR SEPARATION R= 0.50 A.U. TO 10.00 A.U.				
1	.131702E+00	-.672335E-02	.222916E+00	.863263E-02	.598761E-02
2	.249225E+00	.164582E+00	-.115436E+01	-.249055E-01	-.528169E-01
3	-.366194E+00	-.109142E+00	.120355E+01	.951713E-01	.564640E-01
4	.256777E+00	.419659E-01	-.513519E+00	-.908225E-01	-.487190E-01
5	-.108719E+00	-.105361E-01	.895188E-01	.537802E-01	.259916E-01
6	.296660E-01	.176103E-02	.493088E-02	-.186266E-01	-.817477E-02
7	-.532375E-02	-.192613E-03	-.516876E-02	.387650E-02	.157103E-02
8	.623755E-03	.130170E-04	.101013E-02	-.496088E-03	-.187809E-03
9	-.458709E-04	-.468460E-06	-.983486E-04	.384036E-04	.136750E-04
10	.192129E-05	.474976E-08	.493899E-05	-.165455E-05	-.556489E-06
11	-.349195E-07	.116716E-09	-.102039E-06	.305095E-07	.972010E-08
	INTERNUCLEAR SEPARATION R= 0.05 A.U. TO 0.50 A.U.				
1	-.502550E-01	-.529426E-03	-.184894E-03	-.731543E-06	-.337676E-05
2	.242328E+01	.135300E+00	-.236385E+00	.204180E-01	-.235460E-01
3	-.184218E+02	-.158244E+00	-.124098E+00	-.241049E-03	-.152599E-02
4	.119064E+03	.110859E+01	.948862E+00	.217185E-01	.246079E-01
5	-.553684E+03	-.588634E+01	-.443912E+01	-.483877E-01	-.815418E-01
6	.163697E+04	.186450E+02	.135327E+02	.839733E-01	.193014E+00
7	-.307064E+04	-.347721E+02	-.225260E+02	-.112823E+00	-.237503E+00
8	.247715E+04	.301700E+02	.114408E+02	.538963E-01	-.911444E-01
9	.131307E+04	.934551E+01	.265144E+02	.899593E-01	.780278E+00
10	-.420828E+04	-.413136E+02	-.494020E+02	-.166443E+00	-.104885E+01
11	.241167E+04	.244583E+02	.256725E+02	.842627E-01	.492341E+00

TABLE II

	A	B	C	D	E	F	G
	INTERNUCLEAR SEPARATION R=10.00 A.U. TO 40.00 A.U.						
1	-.107912E+02	.226504E+01	.308354E+01	.220842E+01	.151111E+01	.322981E+01	-.577851E+01
2	.500094E+01	-.933114E+00	-.143577E+01	-.108720E+01	-.112159E+01	-.107436E+01	.135455E+01
3	-.124029E+01	.209674E+00	.192224E+00	.243949E+00	.245107E+00	.227830E+00	-.190338E+00
4	.143106E+00	-.257455E-01	-.165835E-01	-.289188E-01	-.296699E-01	-.269109E-01	.166063E-01
5	-.109592E-01	.196758E-02	.915747E-03	.213380E-02	.222666E-02	.199155E-02	-.876833E-03
6	.532399E-03	-.966932E-04	-.346403E-04	-.104474E-03	-.109844E-03	-.947653E-04	.242422E-04
7	-.173594E-04	.310293E-05	.924455E-06	.346843E-05	.364324E-05	.293450E-05	-.839977E-07
8	.377561E-06	-.645162E-07	-.173775E-07	-.774635E-07	-.807461E-07	-.534393E-07	-.162713E-07
9	-.526617E-08	.834591E-09	.221255E-09	.111689E-08	.114951E-08	.716910E-09	.517361E-09
10	.426751E-10	-.606596E-11	-.172065E-11	-.940432E-11	-.952122E-11	-.483621E-11	-.683656E-11
11	-.152951E-12	.187228E-13	.616957E-14	.351585E-13	.349218E-13	.133148E-13	.349465E-13
	INTERNUCLEAR SEPARATION R= 0.50 A.U. TO 10.00 A.U.						
1	.133341E+01	.434532E-01	.224127E-02	-.469468E-03	-.155147E+00	.129899E+01	-.239260E+01
2	.343648E+00	-.295644E+00	-.107091E-01	.228779E-02	.785052E+00	.494534E+00	-.255778E+00
3	-.490432E+00	.100523E+01	-.413075E-02	.254059E-01	-.174008E+01	-.715373E+00	.434230E+00
4	.244992E+00	-.873116E+00	-.256264E-01	-.517619E-03	.128975E+01	.359592E+00	-.364996E+00
5	-.559209E-01	.405342E+00	.909184E-02	-.347784E-02	-.530319E+00	-.964678E-01	.167545E+00
6	.308637E-02	-.115387E+00	-.230179E-02	.135237E-02	.136775E+00	.121187E-01	-.433802E-01
7	.967541E-03	.211029E-01	.449868E-03	-.258761E-03	-.230365E-01	-.897657E-04	.666036E-02
8	-.260597E-03	-.249042E-02	-.574114E-04	.293270E-04	.253516E-02	-.186192E-03	-.608460E-03
9	.290363E-04	.183397E-03	.434094E-05	-.201106E-05	-.175826E-03	.253550E-04	.311965E-04
10	-.152721E-05	-.766509E-05	-.176144E-06	.775456E-07	.697668E-05	-.145823E-05	-.748039E-06
11	.323732E-07	.138826E-06	.295295E-08	-.129532E-08	-.120755E-06	.324137E-07	.405030E-08
	INTERNUCLEAR SEPARATION R= 0.05 A.U. TO 0.50 A.U.						
1	.141418E+01	-.222297E-05	-.136945E-05	.107291E-04	.251910E-06	.141413E+01	-.244942E+01
2	.222988E-02	.103524E-02	-.276871E-04	.163425E-03	-.998359E-03	.478311E-02	-.352018E-02
3	-.533171E-01	.248699E+00	-.245728E-01	.265154E-01	-.249581E+00	-.114575E+00	.829472E-01
4	.701983E+00	.851858E-01	-.334753E-02	.196229E-01	-.739191E-01	.150956E+01	-.108746E+01
5	-.575567E+01	-.485831E+00	-.491055E-02	-.119813E+00	.317727E+00	-.123439E+02	.881383E+01
6	.300907E+02	.130369E+01	-.174750E-01	.406808E+00	-.819760E+00	.647391E+02	-.464650E+02
7	-.105214E+03	-.269871E+01	.842397E-01	-.968076E+00	.103844E+01	-.226410E+03	.162388E+03
8	.242094E+03	.333223E+01	-.166326E+00	.154939E+01	.567435E+00	.520953E+03	-.373385E+03
9	-.352102E+03	-.189137E+01	.180466E+00	-.156624E+01	-.378164E+01	-.757708E+02	.542866E+03
10	.293400E+03	-.216894E+00	-.101478E+00	.886293E+00	.494945E+01	.631408E+03	-.452242E+03
11	-.106689E+03	.572960E+00	.215805E-01	-.207047E+00	-.230053E+01	-.229604E+03	.164411E+03

TABLE III

	A	B	C	D	E	F	G	H
	INTERNUCLEAR SEPARATION R=10.00 A.U. TO 40.00 A.U.							
1	.125713E+01	.532846E+00	.462262E+00	.235422E+00	.963500E+00	.196376E+00	.305571E+00	-.677512E-01
2	-.225640E+00	-.693540E-01	-.676409E-01	-.198466E-01	-.993970E-01	.227858E-01	-.187303E-01	.218898E+00
3	.371402E-01	.809655E-02	.816330E-02	.147075E-02	.126248E-01	-.513072E-02	.125442E-02	-.485791E-01
4	-.384649E-02	-.782308E-03	-.639786E-03	-.697453E-04	-.106588E-02	.526528E-03	-.611766E-04	.576018E-02
5	.266587E-03	.598106E-04	.341712E-04	.113660E-05	.627202E-04	-.340812E-04	.251234E-05	-.435073E-03
6	-.127127E-04	-.330535E-05	-.127205E-05	.919110E-07	-.262045E-05	.151190E-05	-.954114E-07	.221518E-04
7	.419215E-06	.125642E-06	.330608E-07	-.734648E-08	.776078E-07	-.468666E-07	.313723E-08	-.770316E-06
8	-.940197E-08	-.318154E-08	-.588419E-09	.251462E-09	-.159441E-08	.100062E-08	-.774398E-10	.180426E-07
9	.136960E-09	.512036E-10	.683119E-11	-.477283E-11	.216153E-10	-.140302E-10	.126961E-11	-.272226E-09
10	-.116890E-11	-.473841E-12	-.465340E-13	.488958E-13	-.173882E-12	.116264E-12	-.121131E-13	.238939E-11
11	.443612E-14	.192048E-14	.140745E-15	-.211856E-15	.628411E-15	-.431236E-15	.506535E-16	-.927041E-14
	INTERNUCLEAR SEPARATION R= 0.50 A.U. TO 10.00 A.U.							
1	.212211E+01	.499122E+00	.514069E+00	.222027E+00	.540231E+00	.222150E+00	.234974E+00	.227658E+00
2	-.389916E+00	.569680E-02	-.100544E+00	.136166E-02	-.181503E+00	.340587E-03	-.653740E-01	-.248125E-01
3	.212058E+00	-.490033E-01	-.115545E-02	-.139198E-01	.359497E+00	.201530E-03	.145299E+00	.460584E-01
4	-.271521E-01	.242395E-01	.181298E-01	.678251E-02	-.200234E+00	.540483E-03	-.111982E+00	-.376945E-01
5	.405018E-01	-.723296E-02	-.999400E-02	-.206089E-02	.540546E-01	-.328596E-03	.467900E-01	.182344E-01
6	-.140256E-01	.147300E-02	.297748E-02	.432705E-03	-.722640E-02	.546961E-04	-.121564E-01	-.494420E-02
7	-.309517E-02	-.209207E-03	-.562568E-03	-.632783E-04	.205957E-03	-.130726E-05	.205530E-02	.774244E-03
8	.392070E-03	.200702E-04	.675575E-04	.630878E-05	.763107E-04	-.726325E-06	-.226705E-03	-.703191E-04
9	-.302638E-04	-.125675E-05	-.504397E-05	-.407821E-06	-.114103E-04	.103998E-06	.157481E-04	.347941E-05
10	.130916E-05	.460165E-07	.213291E-06	.153782E-07	.669064E-06	-.594357E-08	-.625652E-06	-.751198E-07
11	-.243420E-07	-.746833E-09	-.390262E-08	-.256386E-09	-.149744E-07	.129439E-09	.108403E-07	.164421E-09
	INTERNUCLEAR SEPARATION R= 0.05 A.U. TO 0.50 A.U.							
1	.200151E+01	.499997E+00	.500194E+00	.222217E+00	.500000E+00	.222213E+00	.222211E+00	.222194E+00
2	.816557E-02	.210919E-03	.106483E-02	.333642E-03	.500603E-03	.554181E-03	.819939E-03	.805769E-03
3	-.283771E+01	-.383884E-01	-.353063E+00	-.178827E-01	.612081E-01	-.110833E-01	.196962E-02	-.863352E-02
4	.712413E+01	.666453E-01	.879747E+00	.105577E+00	.369816E-01	.175300E+00	.224186E+00	.117395E+00
5	-.170514E+02	-.525728E+00	-.228545E+01	-.852954E+00	-.154475E+00	-.142456E+01	-.178021E+01	-.827995E+00
6	.583701E+02	.284784E+01	.816534E+01	.452588E+01	.443634E+00	.752096E+01	.928040E+01	.400312E+01
7	-.201141E+03	-.999529E+01	-.279027E+02	-.158447E+02	-.694103E+00	-.263085E+02	-.322127E+02	-.131989E+02
8	.495411E+03	.230131E+02	.678901E+02	.364580E+02	.212881E+00	.605292E+02	.737043E+02	.291264E+02
9	-.770464E+03	-.334709E+02	-.104782E+03	-.530293E+02	.111215E+01	-.880418E+02	-.106786E+03	-.410891E+02
10	.677695E+03	.278904E+02	.917683E+02	.441905E+02	-.179915E+01	.733678E+02	.887311E+02	.334537E+02
11	-.257107E+03	-.101416E+02	-.347289E+02	-.160691E+02	.895667E+00	-.266791E+02	-.321947E+02	-.119513E+02

BIBLIOGRAPHY

1. Helbig H.F. and Everhart E., 1965, Phys. Rev., 140, 1715-20.

2. Houver J.C., Fayeton J. and Barat M., 1974, J.Phys. B: Atom. Molec. Phys., 7, 1358-69.

3. Bates D.R., and McCarroll R., 1958, Proc. Roy. Soc. A, 245, 175-183.

4. Bates D.R., Massey H.S.W., and Stewart A.L., 1953, Proc. Roy. Soc. A., 216, 437-458.

5. Bates D.R. and Williams D.A., 1964, Proc. Phys. Soc., 83, 425-433.

6. Smith F.J., 1964, Proc. Phys. Soc., 84, 889-899.

7. Marchi R.P. and Smith F.T., 1965, Phys. Rev., 139, A1025-38.

8. Smith F.T., 1965, J. Chem. Phys., 42, 2419-26.

9. Mott M.F., 1930, Proc. Roy. Soc. A, 126, 259.

10. Massey H.S.W. and Smith R.A., 1933, Proc. Roy. Soc. A, 142, 142-72

11. McCarroll R. and Salin A., 1968, J. Phys. B: Atom. Molec. Phys., 1, 163-71.

12. McCarroll R., Piacentini R.D. and Salin A., 1970, J. Phys. B: Atom. Molec. Phys., 3, 137-48.

13. Chidichimo-Frank M.C. and Piacentini R.D., 1974, J. Phys. B: Atom. Molec. Phys., 7, 548-57.

14. Rosenthal H., 1971, Phys. Rev. Let., 27, 635-8.

15. Gaussorgues C. and Salin A., 1971, J. Phys. B: Atom. Molec. Phys., 4, 503-12.

16. Knudson S.K. and Thorson W.R., 1970, Can. J. Phys., 48, 313-29.

17. Gaussorgues C., Le Sech C., Masnou-Seeuws F., McCarroll R., and Riera A., 1975, J. Phys. B: Atom. Molec. Phys., 8, 239-252.

18. _____ , 1975, J. Phys. B: Atom. Molec. Phys., 8, 253-64.

19. Born M. and Oppenheimer R., 1957, Ann. d. Phys., 84, 457.

20. Bates D.R. and Sprevak D., 1970, J. Phys. B: Atom. Molec. Phys., 3, 1483-91.

21. Bates D.R. and Crothers D.S.F., 1970, Proc. Roy. Soc. A, 315, 465-78.

22. Goldstein H., Classical Mechanics, P. 82, (Addison-Wesley Publishing Co., Inc. 1959).

23. Ferguson A.F., 1961, Proc. Roy. Soc. A, 264, 540-5.

24. Cayford J.K., Fimple W.R., and Unger D.G., 1974, J. Comp. Phys., 15, 81-97.

25. Cayford J.K., Fimple W.R., Unger D.G. and White S.P., 1974, J. Comp. Phys., 16, 259-70.

26. Wind H., 1965, J. Chem. Phys., 42, 2371.

27. Peek J.M., 1965, J. Chem. Phys., 43, 3004.

28. Richardson L.F., 1927, Philos. Trans. Roy. Soc. London Ser. A, 226, 299.

29. McCarroll R. and Piacentini R.D., 1970, J. Phys. B: Atom. Molec. Phys., 3, 1336-45.

30. Ford K.W. and Wheeler J.A., 1959, Ann. Phys. (N.Y.), 7, 259.

31. Fimple W.R. and White S.P., 1975, Int. J. Q. Chem., 9, 301-324.

Contour Diagram of $|\psi|^2$ for $4f\sigma\mu$ taken through the XZ plane.